Simulation-based techno-economic optimization of CO_2 liquefaction processes in Aspen HYSYS

Mustafa Cakartas

Submitted to Department of Chemistry and Bioscience, Aalborg University Esbjerg

AALBORG UNIVERSITY
STUDENT REPORT

Title:	Simulation-based techno-economic optimization of CO_2 liquefaction processes in Aspen HYSYS
Theme:	Master’s Thesis
Thesis Period:	Fall and Spring Semester 2023-2024
Project Group:	CE4-1-F24
Supervisor(s):	Haoshui Yu Anders Andreasen
Copies:	1
Page Numbers:	47
Date of Completion:	2024-05-30

Participant(s):

Mustafa Cakartas

Abstract

Carbon Capture and Storage (CCS) is a good solution to decrease the CO_2 emissions. However, this process involves capture, transportation and storage. This study focuses on the liquefaction process which takes place between capture and transportation stages. The goal of liquefaction is to liquefy the CO_2 to lower the cost of ship-based CO_2 transportation. For this purpose, internal refrigeration, external refrigeration, precooled Linde-Hampson system and Linde dual-pressure system were simulated in Aspen HYSYS with the target pressure of liquid CO_2 at 7 and 15 bar. Based on the simulation in Aspen HYSYS, the systems were optimized by Particle Swarm Optimization (PSO) in MATLAB. The objective function was defined as Levelized Cost of CO_2 Liquefaction (LCOCL). Therefore, liquefaction systems are optimized with respect to their LCOCL values. When the systems and pressures are compared with respect to LCOCL values, it was determined that external refrigeration with target pressure at 15 bar, 19.88 \$/tCO_2 liquefied, is the most economical option which was evaluated in this study whereas internal refrigeration with target pressure at 7 bar, 26.62 \$/tCO_2 liquefied, is the most expensive option. After a case study, it was determined that considering a compressor with multiple stages to calculate the purchase cost of the compressors lowers the LCOCL values to 17.69 \$/tCO_2 liquefied and 24.37 \$/tCO_2 liquefied, respectively.

Preface

This Master's Thesis was completed in the department of Chemistry and Bioscience in Aalborg University Esbjerg under the supervision of Professor Haoshui Yu and co-supervision of Anders Andreasen (Rambøll Group).

The thesis commenced on the 1st of September 2023 and finished on the 30th of May 2024 and it involves the evaluation of several liquefaction systems at two different liquefaction pressures.

I would like to thank my supervisor, Professor Haoshui Yu, and my co-supervisor, Anders Andreasen, for their help and support during the Master's Thesis. Their knowledge and feedbacks guided me through whole process.

Lastly, I would like to thank my family for their support. Their belief motivated me through the thesis. Hence, I achieved to complete the Master's Thesis.

Table of Contents

1 Introduction

Industrial processes and the combustion of fossil fuels are the main contributors of carbon dioxide (CO_2) emissions. CO_2 emissions can be addressed as a serious problem that should be taken into account. Replacing fossil fuels with renewable energy sources is a good solution [1]. However, renewable energy technologies have sporadic structure which prevents renewable energy to entirely substitute the fossil fuel [2]. This drawback of using renewable energy prevents it to be an efficient solution to CO_2 emission. On the other hand, Carbon Capture and Storage (CCS) is also a good solution to that problem as it offers a significant decrease in the CO_2 emissions [1]. The CO_2 emissions in the world and Denmark can be investigated over a certain time frame to determine its alteration.

If we consider the time frame between 2002 and 2022, whereas the carbon emissions increased from 26.25 to 37.15 billion tons in the world, it decreased from 55.55 to 29.06 million tons in Denmark [3]. As it can be seen from the data mentioned, Denmark is a good example that demonstrates the CO_2 emissions can be lowered significantly. Moreover, countries which desire to reduce the CO_2 emissions may take precaution such as using CCS technology.

CCS has three main components which can be listed as capture, transportation, and storage. The capture process can be defined as the separation of CO_2 from a gaseous stream [1]. There are several carbon capture methods used such as pre-combustion, post-combustion, oxy-fuel combustion, chemical looping combustion and direct air capture [4].

Pre-combustion capture involves the capture of CO_2 from fuel before combustion. After the gasification, carbon monoxide (CO) and hydrogen (H_2) are obtained. Later, water shift gas reaction is utilized to obtain CO_2 and H_2 which will be separated. On the other hand, post-combustion capture involves the capture of CO_2 from flue gas after combustion of fuel. There are different methods that can be used for carbon capture. For example, solvent-based absorption, physical separation (adsorption) and membrane separation are useful methods which can be utilized [5].

In addition to pre-combustion and post-combustion capture methods, oxy-fuel combustion capture can be used. It involves the combustion of fuel with the oxygen-enriched stream which is separated from the air. As a result, water vapor and CO_2 form. Separation of CO_2 is provided with the condensation of water vapor [5]. Another capture method is the chemical looping combustion which uses metal oxides as oxygen carriers to oxidize the fossil fuel. As a result of oxidation, CO_2 and H_2O form. Later, capture of CO_2 is provided with the condensation of H_2O [6]. Beside these methods, Direct Air Capture (DAC) can be used. As its name implies, CO_2 is captured from the air in this process [7].

After, the captured CO_2 is transported to storage sites with the use of trucks, ships, or pipelines. The CO_2 is usually kept at underground formations, ocean reservoirs or it is used in manufacturing processes [1].

While pipelines can be used to transport CO_2 at large amounts for short distances, it is important that CO_2 should be compressed above 73.8 bar which is the critical pressure of CO_2. On the other hand, CO_2 is advised to be transported between 6 and 15 bar in ship transportation above its triple point [8]. It should be noted that the triple point of CO_2 (5.18 bar, -56.6 °C) [9] is important as formation of dry ice is possible at pressures in the vicinity of triple point [10].

Utilizing ship for transportation of CO_2 offers higher flexibility compared to pipeline since route and capacity can be altered according to demand [4]. When the transportation of 1 tonne CO_2 over 1 km is compared for systems which can transport 10 Mtpa (Million tonnes per annum), it was found that after approximately 750 km, ship transportation becomes more economical than the offshore pipeline (50% capacity is used) and onshore pipeline (50% capacity is used) [11]. In the study of Decarre et al. [12], it was found that ship is more economical option than offshore pipeline for CO_2 transportation above 350 km. Moreover, it also becomes more economical than onshore pipeline above 1100 km. Therefore, it can be concluded that ship transportation is an appealing choice for long-distance transportation of CO_2. To reduce the cost of ship-based transportation, the captured CO_2 should be transformed from gas to liquid [13]. Moreover, liquefaction of CO_2 enables the transportation of higher amount since the density of liquefied CO_2 is higher than gaseous CO_2 [14]. This leads liquefaction to play an important role in the conditioning of CO_2 before transportation. Liquefaction can be completed in different ways which can be categorized as open and closed liquefaction systems.

In open liquefaction systems, CO_2 is compressed before it is cooled through a valve. Joule-Thomson effect which occurs during expansion, enables CO_2 to present in the form of a liquid-gas mixture. Afterwards, liquefied CO_2 is separated from a mixture with the use of a flash separator. In this method, there is no need for refrigerant to obtain liquefied CO_2 [13].
The Joule-Thomson effect occurs during the expansion of real gases at constant enthalpy. Joule-Thomson inversion temperature and process's temperature affect the Joule-Thomson coefficient.

When the coefficient is positive, cooling occurs. On the other hand, when the coefficient is negative, heating occurs. CO_2 is an example of gases that experiences cooling effect at room temperature [15].

On the other hand, the use of refrigerant is needed to obtain the liquefied CO_2 in external refrigeration. In this scheme, refrigerant provides an efficient cooling to liquefy CO_2 [16].

Beside internal and external refrigeration, Linde dual-pressure and precooled Linde-Hampson systems are also valuable options for liquefaction. In the Linde dual-pressure system, two stage compression is used. CO_2 is compressed to an intermediate and higher-pressure stages gradually. In between compression stages, intercooling is used to lower the temperature of CO_2 stream. Furthermore, in the precooled Linde-Hampson system, CO_2 is cooled before it is sent to a valve where Joule-Thomson effect provides liquefaction. This precooling increases the performance of the system. Not only the refrigerant but also the vapor CO_2 which separated from liquid-gas mixture are used in cooling [13].

CCS is a good option to lower carbon emissions, but its techno-economic feasibility is still being investigated. Especially, there are lots of studies conducted related to liquefaction methods to determine the optimum transport pressure and liquefaction method. There are no consistent results as different valuable insights obtained at each study conducted until today. Studies differentiate from each other as some of them focuses on liquefaction pressures and others focuses on liquefaction methods. Also, there are some studies considering both factors. Besides, the use of different refrigerants was investigated in some studies.

When the same liquefaction system is used to test pressures ranging from 7 to 70 bar in Deng et al. [17], liquefaction at 7 bar was found as the most expensive pressure. On the other hand, most economically friendly option was determined as 40-50 bar. The study of Decarre et al. [12] argued that 15 bar is cheaper than 7 bar for CO_2 transportation by ship. Also, Gong et al. [18] claimed when 7 and 15 bar are compared, 15 bar found as cheaper option. However, Roussanaly et al. [19] has different results as 7 barg shipping was found cheaper compared to 15 barg shipping of CO_2.

Øi et al. [16] studied on external refrigeration with ammonia and internal refrigeration at 7 bar. As a result, it was found that the cost of external refrigeration with ammonia is less than the cost of internal refrigeration. Also, four different liquefaction systems which can be listed as closed system, Linde-Hampson system, Linde dual-pressure system and precooled Linde-Hampson system were compared in the study of Seo et al. [13] to compare the life cycle costs. Whereas the lowest life cycle cost was obtained for closed system, the precooled Linde-Hampson system has the lowest life cycle cost among the open systems. Furthermore, Chen and Morosuk [8] conducted a study at the liquefaction pressure of 15 bar and it was claimed that the precooled Linde-Hampson system costs less than the closed systems which use different refrigerants such as ammonia, propane and R134a.

As it can be seen from previous studies, there are different results related to liquefaction pressures and systems. In this thesis, internal refrigeration (IR), external refrigeration (ER), precooled Linde-Hampson system (PLH) and Linde dual-pressure system (LDP) will be investigated at the liquefaction pressures of 7 and 15 bar.

2 Methodology

In this section, modelling, cost assessment and optimization processes will be explained. The modelling section includes the flowsheets of liquefaction systems and assumptions. In the cost assessment section, cost calculation method will be explained. Furthermore, optimization process will be explained in the optimization section.

2.1 Modelling

Internal refrigeration, external refrigeration, precooled Linde-Hampson system, and Linde dual-pressure system were evaluated at 7 and 15 bar, since ship-based transportation was chosen in this study. The flowsheets of liquefaction systems were developed in Aspen HYSYS v9. Moreover, the Peng-Robinson equation of state was used as the thermodynamic property method. The feed obtained after the carbon capture process was assumed as 50 t/h pure CO_2 operating at 1.5 bar and 40 °C. In reality, the stream would include certain amount of impurities after the capture process. However, these impurities are neglected in the base cases and the impact of impurities was investigated separately as a case study.

Ammonia was used as a refrigerant in the base cases since it has low consumption of power [20]. Also, the use of propane was evaluated as a case study. After completing all of the base cases, they were compared according to their technical and economical feasibilities. Especially, Levelized Cost of CO_2 Liquefaction (LCOCL) was chosen at the metric to compare different cases in the cost evaluation.

In the study of Øi et al. [16], a system which utilizes refrigerant was named as external refrigerant since it does not contact with CO_2. Moreover, a system which utilizes the effect of expansion is called as internal refrigeration. The names of systems vary from study to study as Seo et al. [13] named the system which utilizes the refrigerant as a closed system. Moreover, the system which uses the effect of expansion was named as Linde-Hampson system. In this study, systems which use the refrigerant and the effect of expansion were evaluated since they are the two main approaches that can be used for the liquefaction of CO_2 and they were named as internal and external refrigeration. Moreover, precooled Linde-Hampson system [13] which utilizes both of the approaches and Linde dual-pressure [13] which use the idea of Joule-Thomson effect for refrigeration at two pressure level were also investigated since they are worth to evaluate due to their promising nature. All of these systems are derived from the idea of using refrigerant and Joule-Thomson effect. However, it is interesting to evaluate all due to differences in their configurations. This study considers the complexity of these systems with the cost to determine the best liquefaction system.

Table 1. Liquefaction pressure and temperature of liquefaction systems.

Liquefaction Systems	**Pressure (bar)**	**Temperature (°C)**
Internal Refrigeration	7	-48.50
Internal Refrigeration	15	-27.71
External Refrigeration	7	-49
External Refrigeration	15	-28
Precooled Linde-Hampson System	7	-48.50
Precooled Linde-Hampson System	15	-27.71
Linde Dual-Pressure System	7	-48.50
Linde Dual-Pressure System	15	-27.71

In Table 1, liquefaction pressure and temperature of systems are listed. Liquefaction temperatures of external refrigeration cases are different from the others because they are user defined. At the outlet of the heat exchanger, they were defined as closest integer values to the ones assigned in other systems.

To obtain the liquefied CO_2 at the desired conditions, certain assumptions were made.

The design assumption made can be listed as;

- Adiabatic efficiency of compressors was set to 80%.
- Maximum compression ratio was chosen as 4.
- Pressure drop was neglected for air coolers and heat exchangers.
- The temperature of hot streams was assumed as 38 °C at the outlet of the air coolers.
- The minimum approach temperature was assumed as 5 °C in heat exchangers while it was assumed as 3 °C in multi-stream heat exchangers.

These assumptions were used to complete the flowsheets of liquefaction systems which can be seen in the figures listed below.

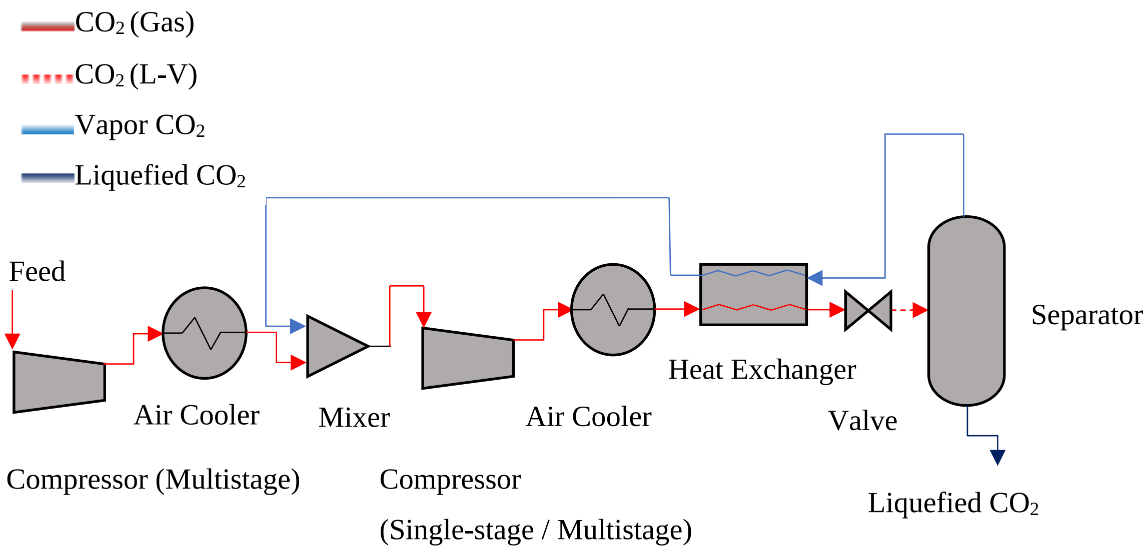

Figure 1. Internal refrigeration flowsheet (adopted from [13]).

Figure 1 represents the internal refrigeration which uses Joule-Thomson effect to liquify the CO_2. In this system, the feed is compressed to high pressures. There are intercooling stages between compressors which regulates the CO_2 stream. Furthermore, air coolers are used for cooling. In the heat exchanger, the hot inlet stream is cooled by the vapor CO_2 which comes from the separator. Later, a valve is used to expand the CO_2 stream to the target pressure. At this stage, the Joule-Thomson effect provides efficient cooling. Hence, CO_2 is transferred from gas to a liquid-vapor mixture and the separator is used to obtain the liquefied CO_2 in the last stage [13].

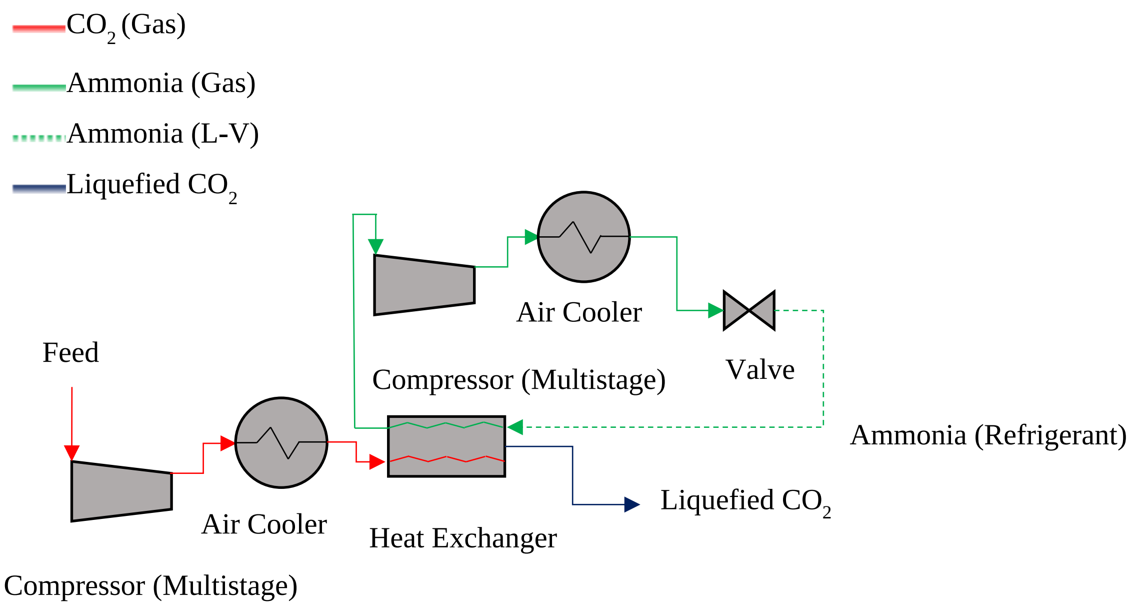

Figure 2. External refrigeration flowsheet (adopted from [13]).

Figure 2 demonstrates the external liquefaction which requires the use of refrigerant to obtain liquefied CO_2. Different from internal refrigeration, feed is directly compressed to the liquefaction pressure. However, intercooling stages exist similar to internal refrigeration. In this study, ammonia is used as a refrigerant in the heat exchanger to obtain the liquefied CO_2 at 49 °C in 7 bar and 28 °C in 15 bar. The inlet conditions of ammonia were determined as 0.3135 bar, -54 °C and 1.0135 bar, -33 °C for 7 and 15 bar cases in this study, respectively. After the heat exchanger, ammonia is compressed and cooled before the valve where expansion leads to the cooling of refrigerant thanks to the Joule-Thomson effect [13].

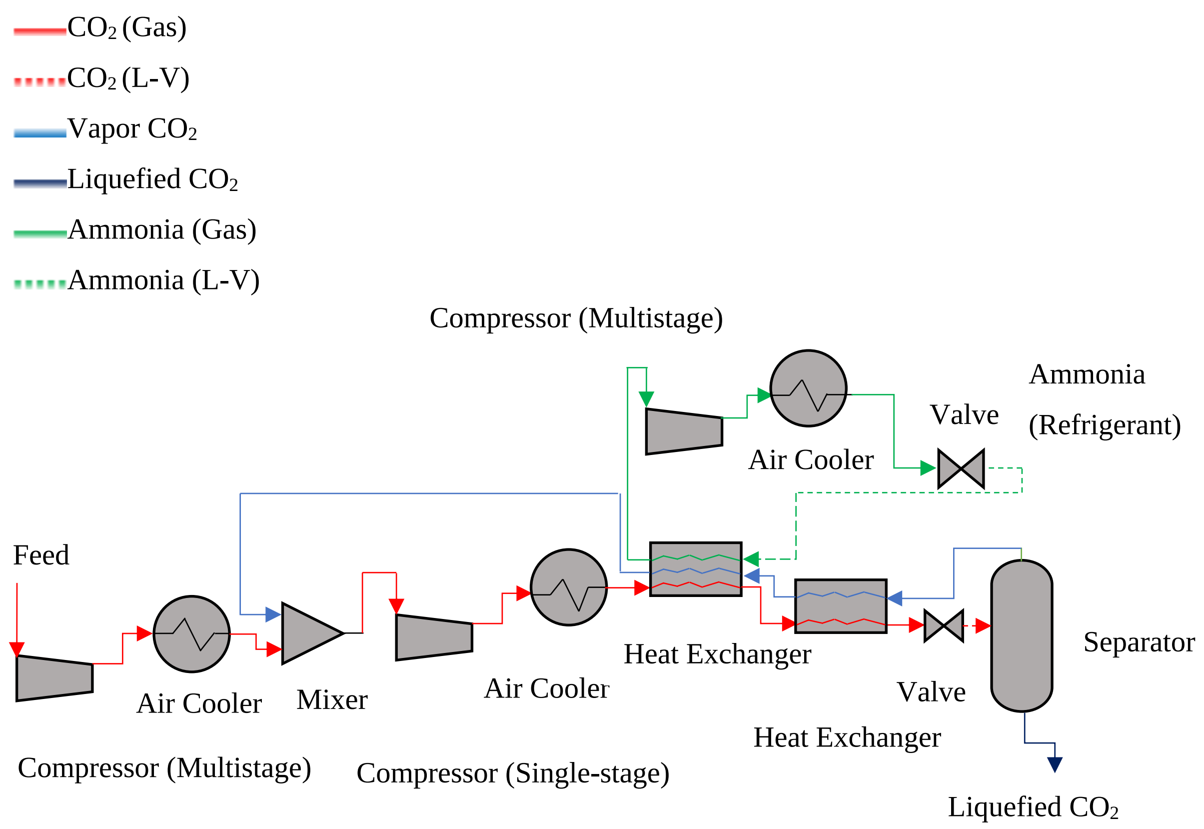

Figure 3. Precooled Linde Hampson system flowsheet (adopted from [13]).

In Figure 3, precooled Linde-Hampson system is illustrated. This liquefaction system is different from the previous ones as the CO_2 stream is cooled by vapor CO_2 and refrigerant. Compressed CO_2 is cooled by the refrigerant and the vapor CO_2 in the first heat exchanger. Later, it is cooled again by vapor CO_2 in the following heat exchanger. Later, valve is used to adjust the pressure to the liquefaction pressure. Moreover, similar to internal liquefaction, Joule-Thomson effect provides cooling which results in obtaining liquid-vapor mixture. Then, mixture is separated and liquefied CO_2 is obtained [13].

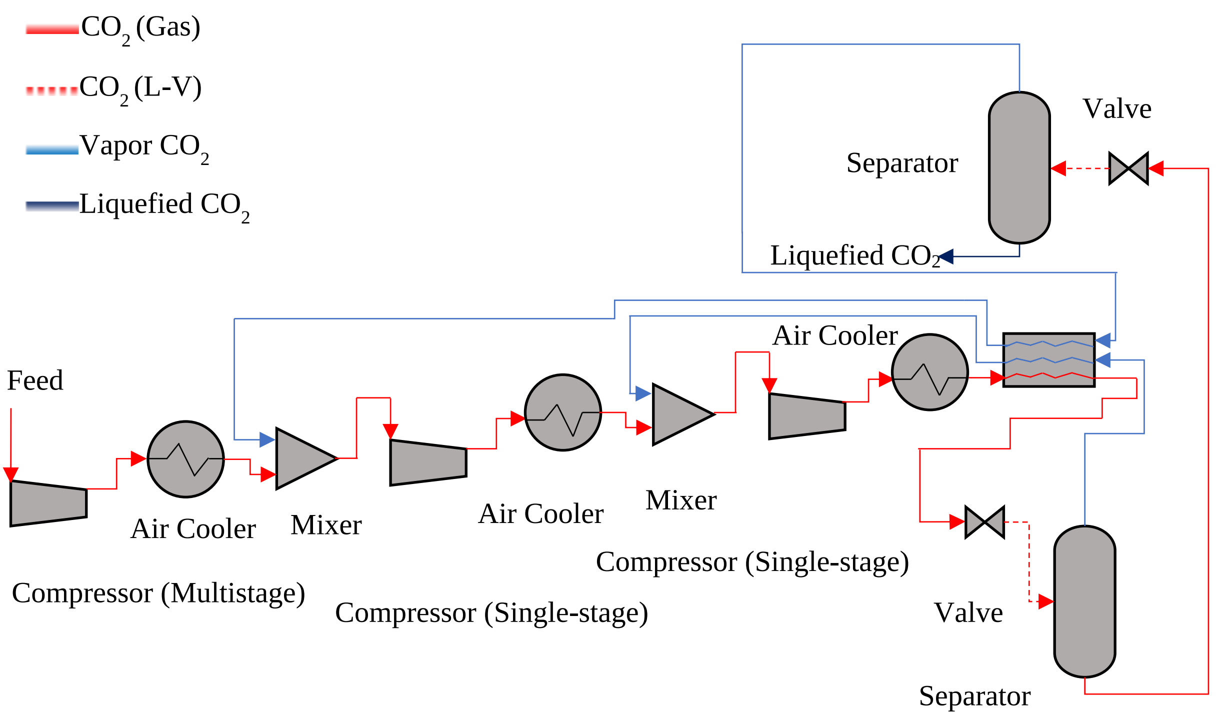

Figure 4. Linde dual-pressure system flowsheet (adopted from [13]).

In Figure 4, the Linde dual-pressure system which is the last liquefaction system considered can be seen. Compressed feed is sent to the mixer where it is mixed with the vapor CO_2 from second separator. It should be noted that the pressure at this stage is the liquefaction pressure. Later, the resulting stream is compressed and sent to a mixer. This stream is mixed with the vapor CO_2 coming from the first separator. Then, the resulting stream is compressed before the heat exchanger. The heat exchanger is used to cool the CO_2 by using the vapor CO_2 streams which come out of the separators. Later, two valves were used to adjust the pressures of streams and provide cooling through expansion. Moreover, two separators were used after the valves to separate the mixtures. As a result, liquefied CO_2 is obtained at the liquefaction pressure [13].

2.2 Cost Assessment

The main purpose of the cost assessment in this thesis is to compare the liquefaction systems and pressures with respect to their LCOCL values. The cost calculations commenced with obtaining the purchase cost of the equipment from the cost database published by Woods [21]. The equipment taken into consideration in the cost calculation are compressors, separators and heat exchangers. Air-cooled heat exchangers (ACHE) have been assumed for coolers, Shell and Tube heat exchangers

(STHE) have been assumed for the heat exchangers, and centrifugal compressors have been assumed for the compressors. To find the purchase cost of these equipment, equation (1) [21] is used.

$$Cost_{2,year} = Cost_{ref} \cdot \left(\frac{size_2}{size_{ref}}\right)^n \tag{1}$$

$Cost_{2,\,year}$ is the cost of the equipment depending on its size in the reference year, $Cost_{ref}$ is the cost of the equipment given by book depending on determined size, $size_2$ is the size of the equipment used to find its purchase cost, $size_{ref}$ is the size provided by the book and n is the power given by book.

The size is power for compressors, area for coolers and heat exchangers, and product of length and diameter to the power of 1.5 for separators. Power of compressors and area of heat exchangers are directly obtained from the Aspen HYSYS v9. However, the area of coolers and size of separators are calculated through the following equations. Equation (2) [22] is used to find the heat transfer area

$$A = \frac{q}{U \cdot \Delta T_m} \tag{2}$$

where A is heat transfer area, q is the heat transfer rate U is the overall heat transfer coefficient and ΔT_m is the mean temperature difference. Instead of mean temperature difference, logarithmic mean temperature difference can be used to determine the area. The logarithmic mean temperature difference can be calculated by using the equation (3) [22]:

$$\Delta T_{lm} = \frac{\Delta T_1 - \Delta T_2}{ln\frac{\Delta T_1}{\Delta T_2}} \tag{3}$$

where ΔT_{lm} is the log mean temperature difference, ΔT_1 is the difference between hot inlet temperature and cold outlet temperature for the countercurrent flow. On the other hand, it is the difference between hot inlet temperature and hot outlet temperature in the cocurrent flow. ΔT_2 is the difference between hot outlet temperature and cold inlet temperature for the countercurrent flow. Moreover, it is the difference between hot outlet temperature and cold outlet temperature in the cocurrent flow [22].

The diameter of separator was required for cost calculations. For this purpose, a website [23] is used and the calculation methodology of this website is provided between the equation (4) and equation (6).

To determine the diameter of the separator, Souders-Brown Equation, equation (4), which is shown below is used to calculate the maximum allowable vapor velocity [24].

$$V = K\sqrt{\frac{\rho_L - \rho_V}{\rho_V}} \tag{4}$$

Where *V* is the maximum allowable vapor velocity, ρ_L is the density of liquid and ρ_V is the density of vapor. *K* is the value that can be determined with the equation (5) [24]:

$$K = 0.35 - 0.01(P - 100)/100 \tag{5}$$

where *P* is the pressure in psig. Therefore, *K* is found in feet/sec.

Later, the diameter of the vessel can be calculated by using equation (6) [24]:

$$D = \sqrt{\frac{4Q}{\pi V}} \tag{6}$$

Where *Q* is the volumetric flowrate of vapor and *V* is the velocity of vapor. L/D ratio ranges between 3 and 5 [24]. In this study, it was chosen as 3.

The costs are provided with the Chemical Engineering Plant Cost Index (CEPCI) of 1000 in Woods [21]. Therefore, the costs are adjusted with the CEPCI of 816 which belongs to October, 2022 [25]. Equation (7) [26] which can be seen below is used to obtain the costs in October,2022:

$$C_{2022} = C_{2,ref} \cdot \frac{CEPCI_{2022}}{CEPCI_{ref}} \tag{7}$$

C_{2022} represents the cost of equipment in 2022, $C_{2,ref}$ is the cost of equipment calculated using equation (1), $CEPCI_{2022}$ is the Chemical Engineering Plant Cost Index in 2022 and $CEPCI_{ref}$ is the Chemical Engineering Plant Cost Index given by the reference.

After the purchase costs in 2022 are obtained, they were used to find the installed costs thanks to Enhanced Detailed Factor method [27]. The material factor is assumed as stainless steel and carbon steel for equipment handling CO_2 and for equipment handling refrigerant, respectively. The purchase costs and installation factors are for equipment in carbon steel. Therefore, material correction is required for equipment which is assumed as stainless steel. The material correction factors were obtained from the Aromada et al. [27] and used to determine the costs of equipment which handle CO_2. The material conversion factor equation, equation (8), [27] is:

$$C_{Eq.,\ CS} = \frac{C_{other\ mat.}}{f_m} \tag{8}$$

where $C_{Eq.,\ CS}$ is the equipment's cost in carbon steel, $C_{other\ mat.}$ is the equipment's cost in other material and f_m is the material factor.

Later, installation costs were determined for each equipment. Moreover, Capital Expenditures (CAPEX) were determined. Fixed Operating Expenses (OPEX) is determined by assuming that it is the 5% of the CAPEX. Variable OPEX is the cost of electricity consumption in compressors and air coolers. The electricity consumption values were obtained from simulation results in Aspen HYSYS v9 for compressors. Furthermore, it is assumed that 10 kW of electricity is needed to cool 1 MW of hot stream. The electricity consumption is multiplied with the electricity cost which was assumed as 0.07 $/kWh with operating hours being 8000 hr/y. As a result of summing up the fixed and variable OPEX, total OPEX was determined. To determine the LCOCL, annualized CAPEX is required. However, Capital Recovery Factor (CRF) should be calculated first to determine the annualized CAPEX. CRF can be calculated by using the equation (9) [28].

$$CRF = \frac{i(1+i)^n}{(1+i)^n - 1} \tag{9}$$

where interest rate is shown with i and number of annuities over the project lifetime is represented with n. Interest rate and annuities over the project lifetime are assumed as 10% and 20 years, respectively.

By using the description made by Short et al. [28] about the NREL's Levelized Cost of Energy (LCOE) methodology, an interpretation of levelized cost is used. The Levelized Cost of CO_2 Liquefaction (LCOCL) can be seen in equation (10) as:

$$LCOCL = \frac{CRF \cdot TPC + O\&M_{fixed} + O\&M_{variable}}{\int_{t=0}^{1\,year} \dot{m}} \tag{10}$$

where *CRF* is the capital recovery factor, *TPC* is the overnight capital cost, $O\&M_{fixed}$ is the fixed Operations and Maintenance cost which is independent of plant load and $O\&M_{variable}$ is the Operations and Maintenance cost which is plant load dependent. The denominator is the nominal mass flow (kg/s) of CO_2 liquefied integrated over the year.

2.3 Optimization

Similar to the approach of Yu et al. [29], the Particle Swarm Optimization (PSO) method is used for optimization. The behaviour of birds, moving as flock, influenced the formation of PSO which is a population based method [30]. PSO is useful optimization method that can be utilized to handle with global optimization problems [31].

The optimization process is completed by using MATLAB. The flowsheets of liquefaction systems are connected to the MATLAB through a COM interface. The objective function is used to optimize the systems similar to method utilized in the studies of Andreasen [32] and Olsen et al. [33]. In Figure 5, the optimization process can be seen.

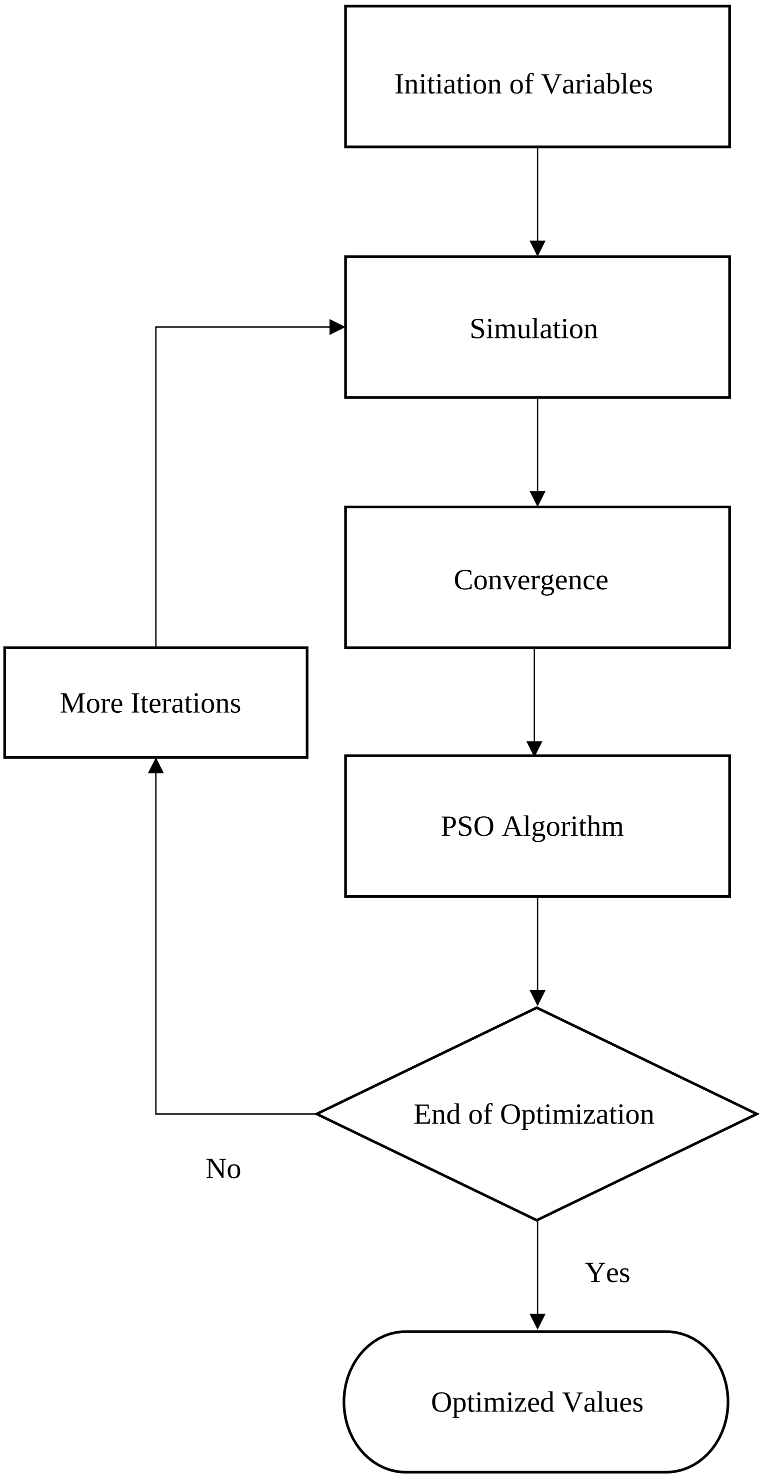

Figure 5. Structure of PSO Algorithm (adopted from [29]).

The optimization starts with the initialization of variables which were defined with their lower and upper boundaries according the certain constraints. The main constraints taken into consideration are obtaining the product with a vapor fraction of 0 and obtaining the vapor fraction of ammonia as 0 at the outlet of heat exchangers since the compressors does not work with liquids. However, the constraints are not used in coding. Instead, they are used to determine the lower and upper boundaries. The values of variables alter in simulations. Moreover, simulation converges if there is no violation. The function tolerance was set as 0.0001. After the optimization process ends, the optimized result is obtained. In this study, the objective function was defined as the LCOCL. Hence, optimized LCOCL is obtained after the process ends. The variables chosen for each liquefaction system can be seen in the following tables with their lower and upper boundaries.

Table 2. Variables and their boundaries in Internal refrigeration.

Liquefaction Pressure (bar)	**Variables (Outlet Pressures)**	**Lower Boundaries (bar)**	**Upper Boundaries (bar)**
7	Low-Pressure Compressor	3	6
	Intermediate-Pressure Compressor	24	28
	First High-Pressure Compressor	70	90
	Second High-Pressure Compressor	140	180
15	Low-Pressure Compressor	3.75	6
	Intermediate-Pressure Compressor	30	60
	High-Pressure Compressor	100	120

Table 3. Variables and their boundaries in External refrigeration.

Liquefaction Pressure (bar)	**Variables (Outlet Pressure)**	**Lower Boundaries (bar)**	**Upper Boundaries (bar)**
7	Low-Pressure Compressor (CO_2)	3	6
	First Low-Pressure Compressor (Refrigerant)	1.01	1.25
	Second Low-Pressure Compressor (Refrigerant)	3.65	5
15	Low-Pressure Compressor (CO_2)	3.75	6
	First Low-Pressure Compressor (Refrigerant)	2.38	4.05
	Second Low-Pressure Compressor (Refrigerant)	6	10

Table 4. Variables and their boundaries in precooled Linde-Hampson system.

Liquefaction Pressure (bar)	**Variables (Outlet Pressure)**	**Lower Boundaries (bar)**	**Upper Boundaries (bar)**
7	Low-Pressure Compressor (CO_2)	3	6
	Intermediate-Pressure Compressor (CO_2)	26.7	28
	Low-Pressure Compressor (Refrigerant)	4	8
15	Low-Pressure Compressor (CO_2)	3.75	6
	Intermediate-Pressure Compressor (CO_2)	29.3	38
	Low-Pressure Compressor (Refrigerant)	4	8

Table 5. Variables and their boundaries in Linde dual-pressure system.

Liquefaction Pressure (bar)	Variables (Outlet Pressure)	Lower Boundaries (bar)	Upper Boundaries (bar)
7	Low-Pressure Compressor	3	6
	Intermediate-Pressure Compressor	22	24
	High-Pressure Compressor	85	88
15	Low-Pressure Compressor	3.75	6
	Intermediate-Pressure Compressor	35	45
	High-Pressure Compressor	90	110

As it can be seen from Table 2, Table 3, Table 4, and Table 5, the variables were chosen as the outlet pressure of the compressors. Compressors are the main contributors of the CAPEX which highly influences the LCOCL. Among the all equipment evaluated, compressors are the most expensive equipment. The boundaries of variables are chosen according to not violating the constraints and assumptions made for compressors. The boundaries of variables are chosen in the valid range to converge the simulation. After observations and trial and error processes, the range is shrunk to decrease the time required for optimization.

3 Case Studies

Case studies were chosen to evaluate alternative cases technically and economically. In this paper, four different case studies were evaluated. Case A is an alternative way which can be used in economic calculations whereas other cases are alternative ways to complete flowsheets of liquefaction systems.

3.1 Case A

Case A is the first case evaluated in this study. In the base cases, cost of the compressors was determined according to their power. Furthermore, each compressor's cost was determined separately. However, determining the cost of a compressor with multiple stages is evaluated in the case study. In this approach, a compressor with multiple stages is assumed and the powers of compressors summed up to find a total power consumption to determine the cost. Compressors are categorized according to the fluids they handle with. Therefore, compressors which handle with CO_2 is evaluated separately from the ones which handle with the refrigerant.

3.2 Case B

In Case B, using an alternative refrigerant in the external refrigeration at the liquefaction pressure of 15 bar is studied. Whereas ammonia is used in the base case, propane is used in the case study to see the effect of refrigerant on the LCOCL. The inlet conditions of propane were determined as 1.49 bar and -33 ℃. The inlet pressure of propane is higher than the inlet pressure of the ammonia at -33 ℃. Furthermore, after the propane at the outlet of heat exchanger is compressed, the temperature of stream was determined as less than 38 ℃. Therefore, the intercooling stage was removed. Also, one more compressor and cooler was removed from the flowsheet since two compressors are enough to reach the target pressure required to obtain the propane at the desired inlet conditions.

3.3 Case C

This case involves the use of ethane and propane as a refrigerant to obtain the liquefied CO_2 at 7 bar in external refrigeration. In the base case, ammonia was used as a refrigerant. However, ammonia has a low vapor pressure at the temperature required to liquefy the CO_2. At -54 ℃, the pressure of ammonia was 0.3135 bar which is less than the atmospheric pressure. Hence, it can cause technical challenges to have the pressure of ammonia at vacuum. On the other hand, using ethane and propane [9] is a prospective solution method. The flowsheet of this case can be seen in Figure 6.

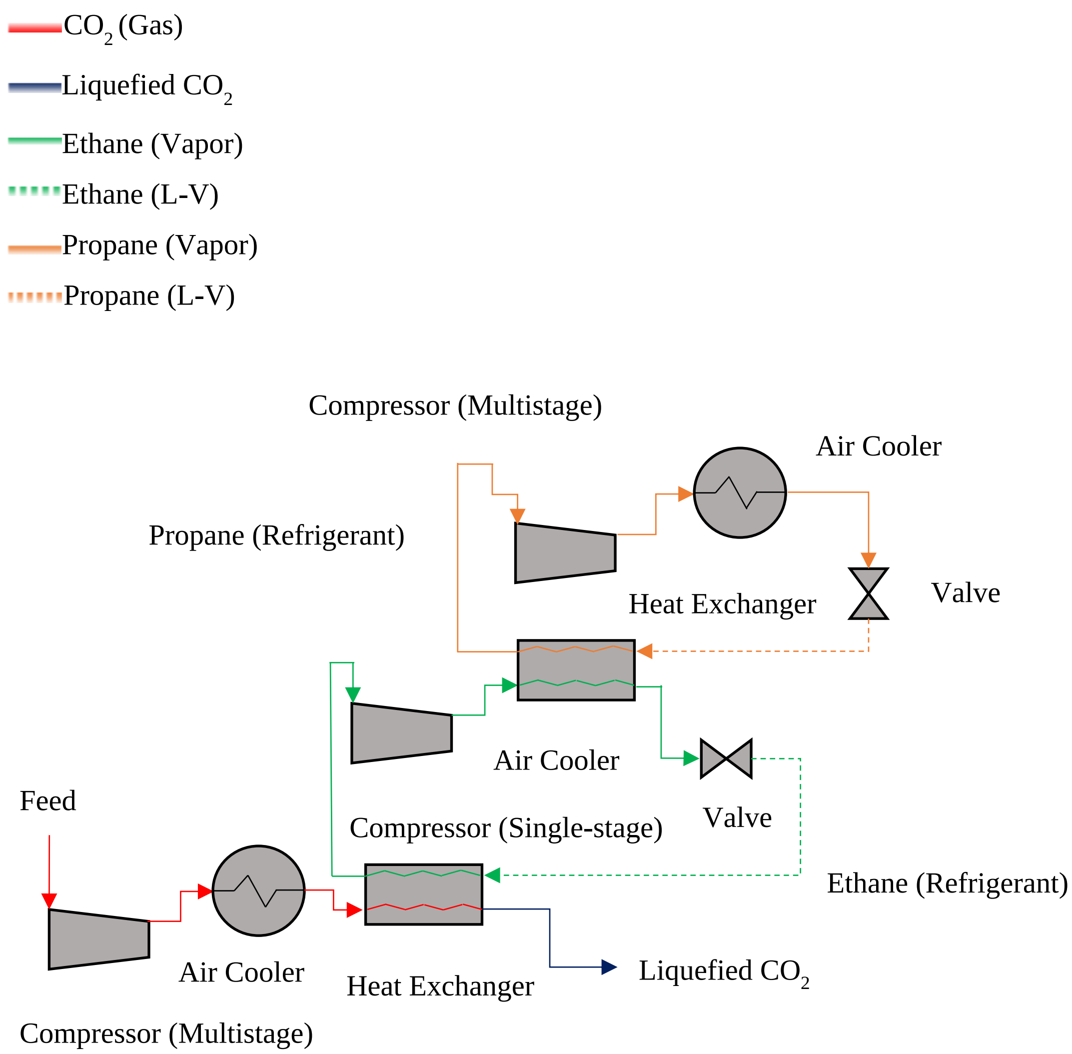

Figure 6. Flowsheet of Case C (adopted from [9]).

As Figure 6 demonstrates, ethane is used to liquefy the CO_2. The inlet pressure of ethane was determined as 4.774 bar at -54 °C in this study. Later, ethane is compressed before it is sent to the heat exchanger where it is cooled by propane. After cooling, it is sent to valve to provide expansion and further cooling of ethane. Also, propane is compressed and cooled before it is sent to a valve and the inlet conditions are reached [9]. In this case study, two refrigerants are used, so there are two different refrigeration cycles.

3.4 Case D

In the last case study, the effect of impurities in the feed stream is investigated. In this study, it was assumed that the carbon capture is completed by using post-combustion capture method and the carbon is captured from a refinery with the technology of membrane. Moreover, the composition of feed stream is 97% CO_2, 2% N_2, and 1% H_2O [17]. The N_2 (nitrogen) and H_2O (water) are the impurities which can be removed to increase the purity of the liquefied CO_2 stream. The flowsheet used to simulate the process with impurities can be seen in Figure 7.

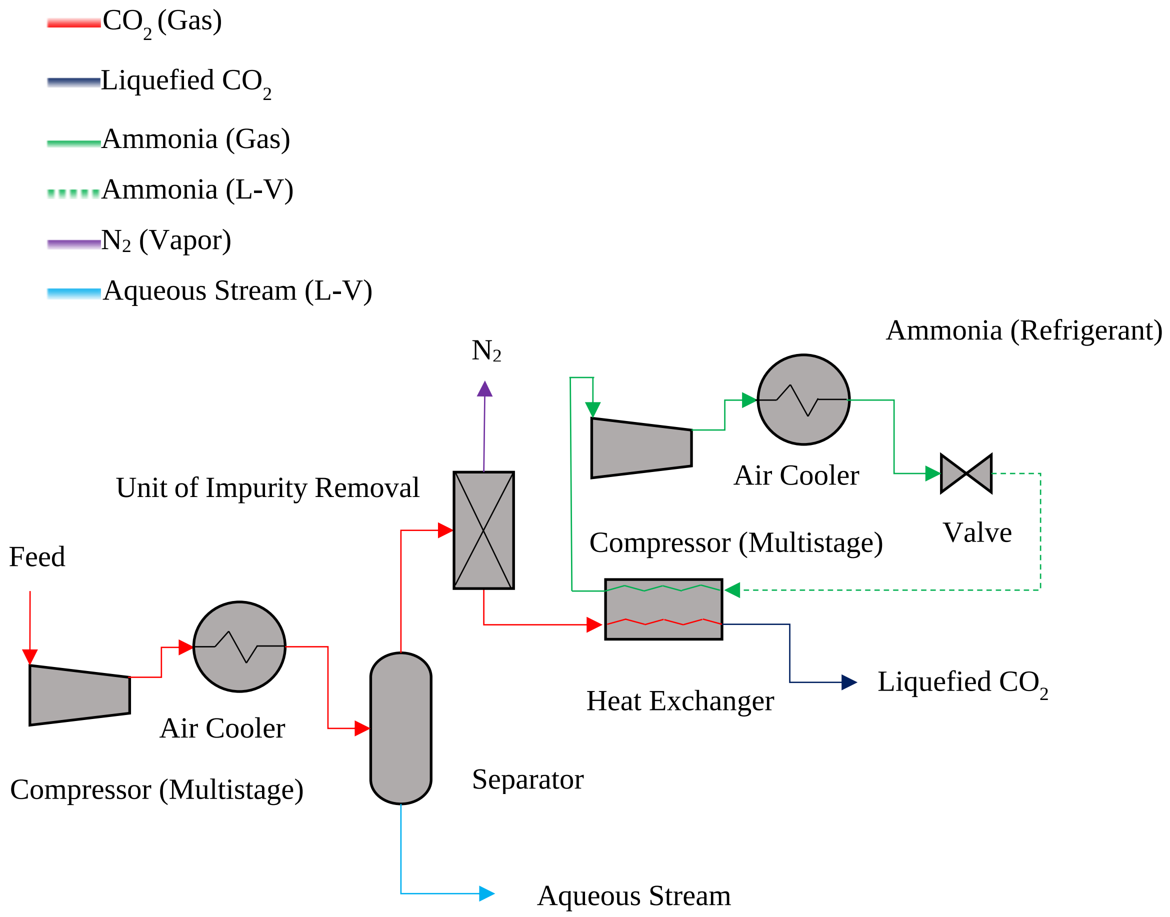

Figure 7. Flowsheet of External refrigeration with impurities (adopted from [17]).

In Figure 7, separator is used to remove the aqueous stream which mostly consists of water. Therefore, certain amount of water can be removed with the separator [17]. Moreover, impurity removal unit is simulated with component splitter in Aspen HYSYS v9. Also, it was assumed that all of the N_2 content is removed through the removal unit. After, the removal of water and nitrogen, the liquefied CO_2 stream has 99.45% CO_2 and 0.55% H_2O.

4 Results and Discussion

In this section, technical, optimization and economic results of base cases will be demonstrated. Later, economic results of case studies will be presented. Lastly, economic results of base cases and case studies will be compared.

4.1 Technical Results

In the liquefaction systems, the amount of CO_2 recycled is different from one to another. The amount of CO_2 recycled and refrigerant used can be seen in the Table 6.

Table 6. Technical results of base cases.

Liquefaction Pressure (bar)	**Liquefaction Systems**	**Mass flow rate of CO_2 recycled (t/h)**	**Mass flow rate of refrigerant used (t/h)**
7	Internal Refrigeration	40.21	-
	External Refrigeration	-	20.68
	Precooled Linde-Hampson System	14.23	16.60
	Linde Dual-Pressure System	12.83	-
15	Internal Refrigeration	43.07	-
	External Refrigeration	-	17.56
	Precooled Linde-Hampson System	8.66	14.74
	Linde Dual-Pressure System	17.51	-

In Table 6, it can be seen that internal refrigeration systems have the highest amount of CO_2 sent back because the pressure of stream before valve should be increased significantly to decrease the amount of liquid. In Addition, external refrigeration systems have the highest amount of refrigeration use since the liquefaction is only provided with the refrigerant. On the other hand, it can be seen that both the amount of recycled CO_2 and amount of refrigerant is low in precooled Linde-Hampson process. Therefore, it can be said that use of refrigerant and recycled CO_2 for liquefaction is a valuable approach.

4.2 Optimization Results

The optimized values determined by using PSO Algorithm in MATLAB can be found in this section. The optimized values obtained for variables are presented in the following tables.

Table 7. Optimized variables in Internal refrigeration.

Liquefaction Pressure (bar)	Variables (Outlet Pressure)	Optimized Values (bar)	Objective Function ($/tons of CO_2 liquefied)
7	Low-Pressure Compressor	6.00	26.62
	Intermediate-Pressure Compressor	24.01	
	First High-Pressure Compressor	86.55	
	Second High-Pressure Compressor	173.06	
15	Low-Pressure Compressor	6.00	23.98
	Intermediate-Pressure Compressor	31.25	
	High-Pressure Compressor	110.60	

Table 8. Optimized variables in External refrigeration.

Liquefaction Pressure (bar)	Variables (Outlet Pressure)	Optimized Values (bar)	Objective Function ($/tons of CO_2 liquefied)
7	Low-Pressure Compressor (CO_2)	6.00	21.58
	First Low-Pressure Compressor (Refrigerant)	1.25	
	Second Low-Pressure Compressor (Refrigerant)	4.31	
15	Low-Pressure Compressor (CO_2)	5.97	19.88
	First Low-Pressure Compressor (Refrigerant)	2.60	
	Second Low-Pressure Compressor (Refrigerant)	9.96	

Table 9. Optimized variables in precooled Linde-Hampson system.

Liquefaction Pressure (bar)	Variables (Outlet Pressure)	Optimized Values (bar)	Objective Function ($/tons of CO_2 liquefied)
7	Low-Pressure Compressor (CO_2)	6.00	23.80
	Intermediate-Pressure Compressor (CO_2)	27.99	
	Low-Pressure Compressor (Refrigerant)	6.03	
15	Low-Pressure Compressor (CO_2)	5.98	22.47
	Intermediate-Pressure Compressor (CO_2)	31.42	
	Low-Pressure Compressor (Refrigerant)	6.63	

Table 10. Optimized variables in Linde dual-pressure system.

Liquefaction Pressure (bar)	Variables (Outlet Pressure)	Optimized Values (bar)	Objective Function ($/tons of CO_2 liquefied)
7	Low-Pressure Compressor	6.00	24.94
	Intermediate-Pressure Compressor	22.27	
	High-Pressure Compressor	88.00	
15	Low-Pressure Compressor	5.77	23.91
	Intermediate-Pressure Compressor	39.28	
	High-Pressure Compressor	95.05	

Table 7, Table 8, Table 9, and Table 10 include the optimized values of variables. Outlet pressures of streams leaving the compressors are varied in this study. After the optimization process, results obtained for all variables were listed. When the optimized values are investigated, it can be seen that some of the variables are chosen at lower and upper boundaries. At this point, it should be noted that exceeding these boundaries might contravene the constraints and assumptions made. These values influence the power of compressors which is used to determine the purchase cost of compressors. At the first glance, it can be thought that lower boundaries should be chosen to decrease the purchase cost. However, the installation factors increases as purchase cost decreases in the EDF method [27]. Hence, it can be seen that upper boundaries were chosen for some variables. Optimum values were determined by taking into account the trade-off between installed costs of equipment which affect the CAPEX and power of compressors which affect the variable OPEX.

4.3 Economic Results

This section involves the results obtained after the optimization process. The economic results will be investigated for base cases and case studies. Later, the comparison will be made.

4.3.1 Economic Results of Base Cases

There are four different liquefaction systems which were evaluated at 7 and 15 bar. In the Table 11, economic results obtained for each system at liquefaction pressures can be seen.

Table 11. Economic results of base cases.

Liquefaction Pressure (bar)	Liquefaction Systems	CAPEX (MM $)	OPEX (MM $/y)	LCOCL ($/tons of CO_2 liquefied)
7	Internal Refrigeration	38.67	6.00	26.62
	External Refrigeration	30.33	4.99	21.58
	Precooled Linde-Hampson System	37.69	4.99	23.80
	Linde Dual-Pressure System	34.20	5.87	24.94
15	Internal Refrigeration	35.23	5.37	23.98
	External Refrigeration	29.53	4.41	19.88
	Precooled Linde-Hampson System	36.45	4.61	22.47
	Linde Dual-Pressure System	37.09	5.11	23.91

Table 11 shows that all of the liquefaction systems have lower LCOCL values at 15 bar. Moreover, when the systems are compared, the trend is same for 7 and 15 bar. Ascending order of LCOCL results are external refrigeration, precooled Linde-Hampson system, Linde dual-pressure system and internal refrigeration. The highest LCOCL value of internal refrigeration can be related to the high recycle amount shown in Table 6. On the other hand, it can be said that external refrigeration seems the most economic liquefaction option with the use of ammonia. The lowest LCOCL value of external refrigeration can be related to the fact that the system does not operate at high pressures, so the cost of compressors which influences the CAPEX dramatically are not as high as they were at other liquefaction systems.

4.3.2 Economic Results of Case Studies

The case studies were completed after base cases to find alternative ways to overcome technical challenges and reduce the cost. The economic results of case studies can be seen in Table 12, Table 13, Table 14, and Table 15.

Table 12. Economic results of Case A.

Liquefaction Pressure (bar)	Liquefaction Systems	CAPEX (MM $)	OPEX (MM $/y)	LCOCL ($/tons of CO_2 liquefied)
7	Internal Refrigeration	33.64	5.71	24.37
	External Refrigeration	26.31	4.74	19.72
	Precooled Linde-Hampson System	33.26	4.72	21.78
	Linde Dual-Pressure System	31.87	5.69	23.79
15	Internal Refrigeration	31.36	5.19	22.37
	External Refrigeration	24.77	4.10	17.69
	Precooled Linde-Hampson System	30.68	4.30	19.98
	Linde Dual-Pressure System	32.81	4.93	22.16

In Table 12, it is clear that all liquefaction systems have lower LCOCL values at 15 bar similar to base cases. The Case A was related to finding the cost of compressors by considering a compressor with multiple stages rather than finding the costs of compressors separately. The finding of Case A is in agreement with base cases in terms of LCOCL ordering as well. Lowest LCOCL was obtained for external refrigeration whereas highest LCOCL was obtained for internal refrigeration.

Table 13. Economic results of Case B.

Liquefaction Pressure (bar)	Liquefaction Systems	CAPEX (MM $)	OPEX (MM $/y)	LCOCL ($/tons of CO_2 liquefied)
15	External Refrigeration	29.15	4.61	20.27
		26.13*	4.45*	18.96*

* These values were obtained by considering a compressor with multiple stages to calculate the costs.

The economic results of Case B can be seen in Table 13. Case B is the study completed by using a propane as a refrigerant for liquefaction in the external refrigeration. There is a certain decrease in LCOCL when the value is found by considering a compressor with multiple stages.

Table 14. Economic results of Case C.

Liquefaction Pressure (bar)	Liquefaction Systems	CAPEX (MM $)	OPEX (MM $/y)	LCOCL ($/tons of CO_2 liquefied)
7	External Refrigeration	32.93	5.64	23.97
		30.68*	5.46*	22.87*

* These values were obtained by considering a compressor with multiple stages to calculate the costs.

Table 14 demonstrates the results obtained for Case C. This case is completed to evaluate the use of propane and ethane instead of ammonia in external refrigeration at 7 bar since the inlet pressure of ammonia is at vacuum. Similar to Case B, considering a compressor with multiple stages in cost calculations decreased LCOCL value.

Table 15. Economic results of Case D.

Liquefaction Pressure (bar)	**Liquefaction Systems**	**CAPEX (MM $)**	**OPEX (MM $/y)**	**LCOCL ($/tons of CO_2 liquefied)**
7	Internal Refrigeration	45.41	6.77	30.56 33.52*
	External Refrigeration	37.22	5.79	25.63 28.59*
	Precooled Linde-Hampson System	44.14	5.78	27.68 30.64*
	Linde Dual-Pressure System	40.92	6.60	28.76 31.72*
15	Internal Refrigeration	35.97	5.40	24.28 27.24*
	External Refrigeration	30.43	4.47	20.32 23.28*
	Precooled Linde-Hampson System	37.23	4.66	22.82 25.78*
	Linde Dual-Pressure System	37.88	5.13	24.21 27.17*

* These LCOCL results were obtained after the cost of removing the impurities are assumed as 500 $/tons of impurities removed. Moreover, in the study of Deng et al. [17], the cost of removal was assumed as 300-500 $/tons of impurities removed.

Table 15 shows the fact that including impurities in the feed stream does not affect the trend of having lowest LCOCL values at 15 bar. Also, the lowest LCOCL value was obtained for external refrigeration and highest value was obtained for the internal refrigeration.

4.3.3 Comparison of Economic Results

LCOCL values obtained in base case will be compared with case studies to see the effect of different methodologies on cost differences.

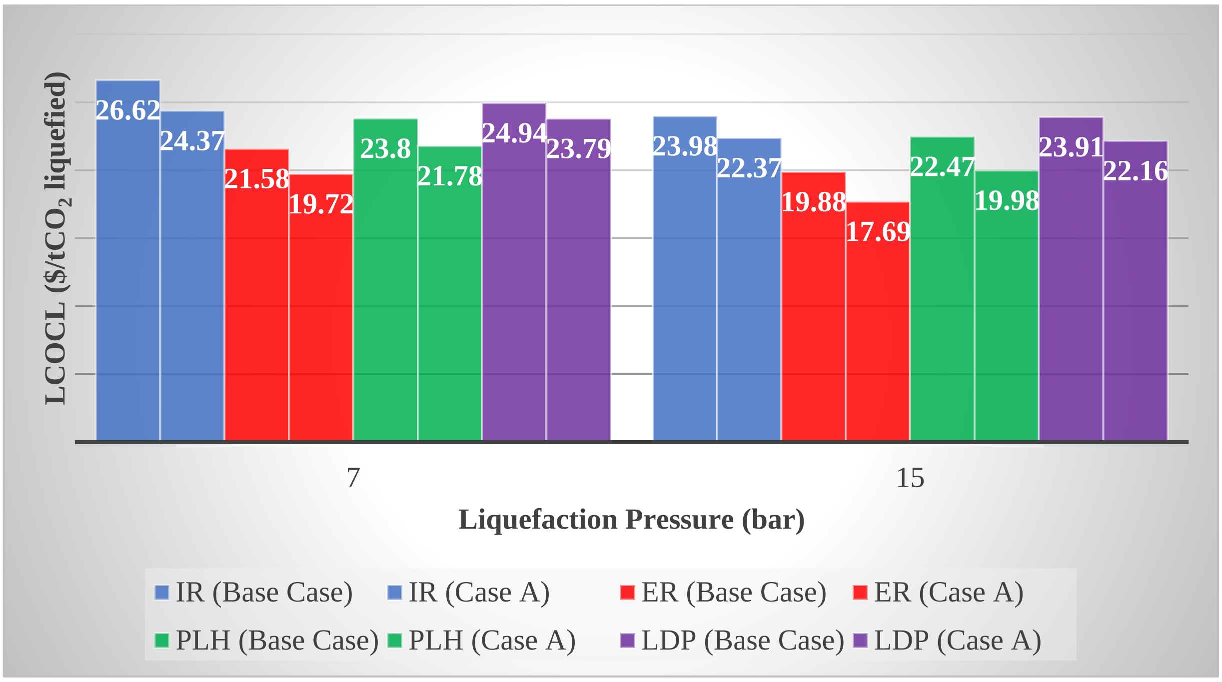

Figure 8. Comparison of LCOCL results of base case and case A.

Figure 8 shows the comparison of LCOCL results for base case and case A. When the results of base case are compared with the case study, it is observed that the LCOCL significantly decreases for all liquefaction systems at 7 and 15 bar when it is calculated by considering a compressor with multiple stages. Hence, it can be said that case A gives more economic results than the base case.

Furthermore, base case and case B were compared with respect to their LCOCL values. In base case, ammonia was used as a refrigerant in external refrigeration. Moreover, propane was used as a refrigerant in the case B. While the LCOCL value of base case is 19.88 $/tCO_2$ liquefied, the value of case B is 20.27 $/tCO_2$ liquefied. The results show that using ammonia instead of propane provides lower LCOCL values. Therefore, using ammonia in external refrigeration is economically beneficial.

In addition, the difference between LCOCL values for base case and case C was determined. In the base case, ammonia was used as a refrigerant in external refrigeration at 7 bar. On the other hand, propane and ethane was used in case C. The LCOCL value of base case is 21.58 $/tCO_2$ liquefied whereas the value of case C is 23.97 $/tCO_2$ liquefied. The difference between LCOCL values show that although using ammonia might be technically challenging, it is economically better option.

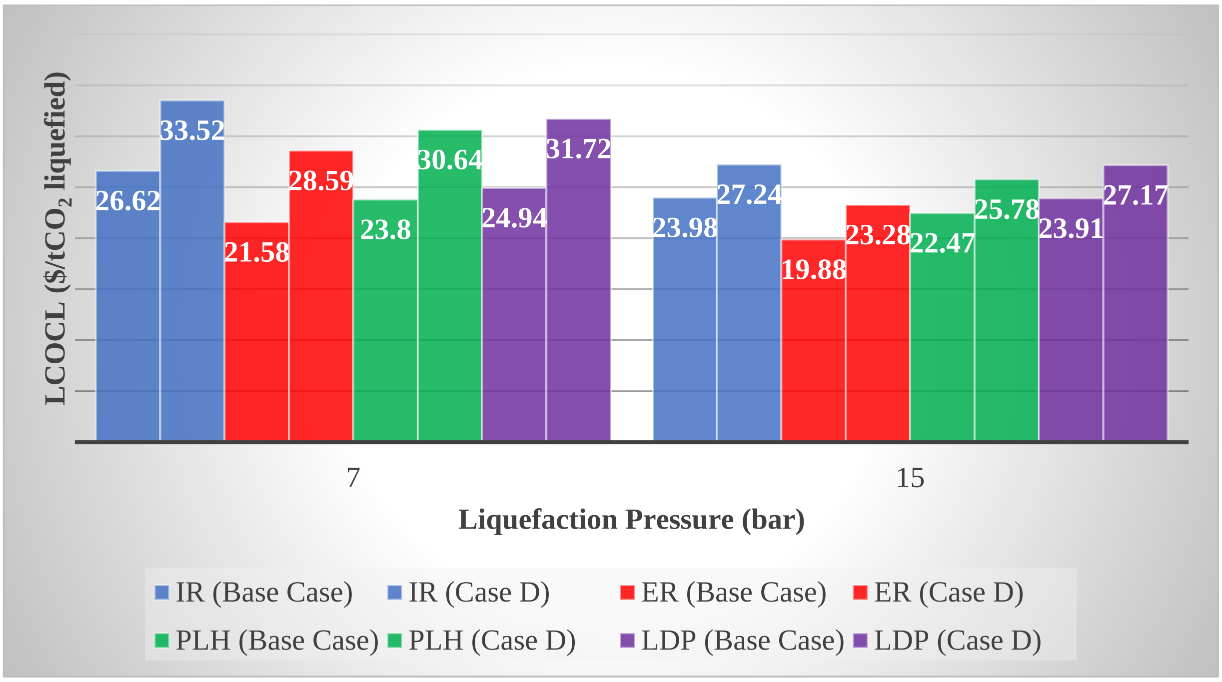

Figure 9. Comparison of LCOCL results of base case and case D.

The comparison of LCOCL results between the base case and case D can be seen in Figure 9. The LCOCL results are clearly higher for case D where impurities present in the feed. LCOCL results of all systems are higher for case D at 7 and 15 bar. However, the difference of LCOCL values between base case and case D is more for 7 bar. In the 7 bar cases, less amount of water was removed compared to 15 bar cases. Therefore, the configurations of 7 bar cases are readjusted and the pressure of streams is increased to 15 bar before impurity removal unit to have the same amount of impurities removed with 15 bar cases. Therefore, this might be the reason of obtaining the LCOCL values of liquefaction systems at 7 bar significantly higher compared to base cases.

4.3.4 Comparison of Economic Results with Other Studies

After determining the costs for base cases, the results were compared with the case studies. Later, they were compared with the results of other studies to see the differences between economic results.

Table 16. Comparison between LCOCL values of base case, Case A and economic results of Seo et al. [13] and Chen and Morosuk [8].

Liquefaction Pressure (bar)	**Liquefaction Systems**	**Base Case**	**Case A**	**Seo et al. [13]**	**Chen and Morosuk [8]**
7	Internal Refrigeration*	26.62	24.37	22.46**	-
	External Refrigeration*	21.58	19.72	18.81**	-
	Precooled Linde-Hampson System	23.80	21.78	17.66**	-
	Linde Dual-Pressure System	24.94	23.79	20.99**	-
15	Internal Refrigeration*	23.98	22.37	19.33	-
	External Refrigeration*	19.88	17.69	16.11	23.32
	Precooled Linde-Hampson System	22.47	19.98	16.27	21.13
	Linde Dual-Pressure System	23.91	22.16	18.65	-

* The internal refrigeration is named as Linde-Hampson system and external refrigeration is named as closed system in the study of Seo et al. [13]. Although the main idea is similar, configurations of closed system and internal refrigeration are designed slightly differently in the study of Seo et al. [13] and in this study. Moreover, external refrigeration is called as three-stage vapor-compression liquefaction system and designed accordingly in the study of Chen and Morosuk [8]. Therefore, although refrigerant is used for liquefaction, designs of systems are different.

** These results were obtained for 6 bar in the study of Seo et al. [13]. They were used for comparison since Seo et al. [13] did not study on 7 bar.

Table 16 shows the LCOCL results of this study and the economic results of other studies. Before starting to interpret the table located above, I would like to clarify that the economic results of Seo et al. [13] were demonstrated in terms of normalized Life Cycle Cost (LCC) in the unit of $/ton. These results were presented in a bar chart. During the reading of values from bar chart, there could be a deviation because ScanIt v2.08 [34] was used to read the points between a scale from 0 to 22.5. Therefore, these results might not be exactly same with the values obtained by Seo et al. [13]. Moreover, Chen and Morosuk [8] presented their results as specific CO_2 liquefaction cost in the unit of $/t$CO_2$. While the cost of precooled Linde-Hampson process was presented in numerical value in the study of Chen and Morosuk [8], the cost of external refrigeration with ammonia was estimated by using ScanIt v2.08 [34] since the cost was presented in the bar chart. Therefore, a deviation might have occurred. In this thesis, base case and case A's results are presented in terms of LCOCL in the unit of $/t$CO_2$ liquefied.

It should be underlined that different optimization and cost calculation methodologies were utilized. For example, while Seo et al. [13] used HYSYS optimizer in precooled Linde-Hampson system, Chen and Morosuk [8] mentioned that multi-objective optimization will be their next step. On the other hand, PSO was implemented to optimize liquefaction systems in this thesis. Moreover, Seo et al. [13] used the Aspen Process Economic Analyzer to obtain the costs of equipment when they were available in it. Also, Aspen Process Economic Analyzer is used by Chen and Morosuk [8] as well. On the other hand, the purchase costs of equipment were obtained from Woods [21] and installed costs were calculated through the EDF method [27] in this thesis.

As it was mentioned before, LCOCL values of case A is lower than the LCOCL results of base case. However, when the LCOCL results of case A and base case are compared with the normalized LCC values of Seo et al. [13], it can be seen that the results of Seo et al. [13] are lower than the results of this study. The differences between results can be related different reasons such as time differences between studies and its possible effect on CEPCI index, differences in the feed flowrates, technical assumptions made and methods used to calculate the costs. However, it can be said that although there are differences between results, the general trend of both studies is quite similar since the lowest cost is obtained for external refrigeration and highest cost is obtained for internal refrigeration at 15 bar. However, Seo et al. [13] determined the lowest cost for precooled Linde-Hampson system at 7 bar whereas it was obtained as external refrigeration in this study.

From the study of Chen and Morosuk [8], the cost comparison can be made for external refrigeration with ammonia and precooled Linde-Hampson system at 15 bar. When the cost differences were investigated for external refrigeration with ammonia at 15 bar, it was found that the base case and case A have lower cost compared to configuration used in Chen and Morosuk [8]. This difference might be caused by the configuration differences and other differences such as assumptions and strategy used to determine the cost. Moreover, when the cost of precooled Linde-Hampson system from the study of Chen and Morosuk [8] is compared with the costs of base case and case A, it was observed that it is lower than the cost of base case but higher than the cost of case A. The differences between cost results might be caused by the reasons mentioned earlier such as assumptions made and ways the costs were calculated.

5 Conclusions

This study was conducted to evaluate the liquefaction systems and liquefaction pressures. While internal refrigeration, external refrigeration, precooled Linde-Hampson system, and Linde dual-pressure systems were selected as the liquefaction systems, 7 and 15 bar were selected as the liquefaction pressures. Among the base cases, external refrigeration proposed the lowest LCOCL values for both 7 and 15 bar. Moreover, internal refrigeration was determined as the most expensive system at both 7 and 15 bar. On the other hand, when 7 and 15 bar are compared, it was observed that 15 bar is more appropriate liquefaction pressure in terms of the LCOCL evaluation since all of the liquefaction systems cost less at 15 bar. When the case studies are completed, it was determined that calculating the purchase cost of compressors by considering a compressor with multiple stages lowers the LCOCL significantly. Also, different refrigerants such as propane, and propane and ethane were considered in external refrigeration system at 15 and 7 bar, respectively. Both of the cases demonstrated that using ammonia as a refrigerant enables to obtain lower LCOCL values. Lastly, presence of impurities was evaluated and it was found that removing the impurities result in higher LCOCL values than base case. All in all, it can be said that using external refrigeration for liquefaction process at 15 bar is the most economical option with respect to LCOCL evaluation.

As a further work, the purchase cost of equipment can be calculated by using different methods and information from literature. Moreover, CAPEX is calculated by using EDF method in this study. However, different methods can be used to calculate the CAPEX which influences the LCOCL. Using different techniques for cost calculations may enable the comparison of these strategies. Also, Particle Swarm Optimization is used in this study to optimize the LCOCL of liquefaction systems, but different optimization algorithms can be used as a future work to see the effect of optimization techniques on the results of LCOCL.

6 References

[1] B. Metz, O. Davidson, H. de Coninck, M. Loos, and L. Meyer, Eds., *IPCC Special Report on Carbon Dioxide Capture and Storage*, 1st ed. New York: Cambridge University Press, 2005.

[2] H. Sultan *et al.*, 'Reducing the efficiency penalty of carbon dioxide capture and compression process in a natural gas combined cycle power plant by process modification and liquefied natural gas cold energy integration', *Energy Conversion and Management*, vol. 244, p. 114495, Sep. 2021, doi: 10.1016/j.enconman.2021.114495.

[3] H. Ritchie, P. Rosado, and M. Roser, 'CO_2 and Greenhouse Gas Emissions', *Our World in Data*, 2023, Accessed: May 18, 2023. [Online]. Available: https://ourworldindata.org/co2-and-greenhouse-gas-emissions

[4] Danish Energy Agency, 'Technology Data for Carbon Capture, Transport and Storage', *Danish Energy Agency and Energinet*, 2021, [Online]. Available: https://ens.dk/sites/ens.dk/files/Analyser/technology_data_for_carbon_capture_transport_and_storage.pdf

[5] P. Madejski, K. Chmiel, N. Subramanian, and T. Kuś, 'Methods and techniques for CO_2 capture: Review of potential solutions and applications in modern energy technologies', *Energies*, vol. 15, no. 3, p. 887, Jan. 2022, doi: 10.3390/en15030887.

[6] H. A. Alalwan and A. H. Alminshid, 'CO_2 capturing methods: Chemical looping combustion (CLC) as a promising technique', *Science of The Total Environment*, vol. 788, p. 147850, Sep. 2021, doi: 10.1016/j.scitotenv.2021.147850.

[7] D. W. Keith, G. Holmes, D. St. Angelo, and K. Heidel, 'A process for capturing CO_2 from the atmosphere', *Joule*, vol. 2, no. 8, pp. 1573–1594, Aug. 2018, doi: 10.1016/j.joule.2018.05.006.

[8] F. Chen and T. Morosuk, 'Exergetic and economic evaluation of CO_2 liquefaction processes', *Energies*, vol. 14, no. 21, p. 7174, Nov. 2021, doi: 10.3390/en14217174.

[9] Y. Seo, C. Huh, S. Lee, and D. Chang, 'Comparison of CO_2 liquefaction pressures for ship-based carbon capture and storage (CCS) chain', *International Journal of Greenhouse Gas Control*, vol. 52, pp. 1–12, Sep. 2016, doi: 10.1016/j.ijggc.2016.06.011.

[10] S. Trædal, J. H. G. Stang, I. Snustad, M. V. Johansson, and D. Berstad, 'CO_2 liquefaction close to the triple point pressure', *Energies*, vol. 14, no. 24, p. 8220, Dec. 2021, doi: 10.3390/en14248220.

[11] 'The Costs of CO_2 Transport: Post-demonstration CCS in the EU'. European Technology Platform for Zero Emission Fossil Fuel Power Plants. Accessed: May 14, 2024. [Online].

Available: https://www.globalccsinstitute.com/archive/hub/publications/119811/costs-co2-transport-post-demonstration-ccs-eu.pdf

[12] S. Decarre, J. Berthiaud, N. Butin, and J.-L. Guillaume-Combecave, 'CO_2 maritime transportation', *International Journal of Greenhouse Gas Control*, vol. 4, no. 5, pp. 857–864, Sep. 2010, doi: 10.1016/j.ijggc.2010.05.005.

[13] Y. Seo, H. You, S. Lee, C. Huh, and D. Chang, 'Evaluation of CO_2 liquefaction processes for ship-based carbon capture and storage (CCS) in terms of life cycle cost (LCC) considering availability', *International Journal of Greenhouse Gas Control*, vol. 35, pp. 1–12, Apr. 2015, doi: 10.1016/j.ijggc.2015.01.006.

[14] B.-Y. Yoo, 'The development and comparison of CO_2 BOG re-liquefaction processes for LNG fueled CO_2 carriers', *Energy*, vol. 127, pp. 186–197, May 2017, doi: 10.1016/j.energy.2017.03.073.

[15] C. M. Oldenburg, 'Joule-Thomson cooling due to CO_2 injection into natural gas reservoirs', *Energy Conversion and Management*, vol. 48, no. 6, pp. 1808–1815, Jun. 2007, doi: 10.1016/j.enconman.2007.01.010.

[16] L. E. Øi, N. Eldrup, U. Adhikari, M. H. Bentsen, J. L. Badalge, and S. Yang, 'Simulation and cost comparison of CO_2 liquefaction', *Energy Procedia*, vol. 86, pp. 500–510, Jan. 2016, doi: 10.1016/j.egypro.2016.01.051.

[17] H. Deng, S. Roussanaly, and G. Skaugen, 'Techno-economic analyses of CO_2 liquefaction: Impact of product pressure and impurities', *International Journal of Refrigeration*, vol. 103, pp. 301–315, Jul. 2019, doi: 10.1016/j.ijrefrig.2019.04.011.

[18] W. Gong, E. Remiezowicz, P. L. Fosbøl, and N. von Solms, 'Design and analysis of novel CO_2 conditioning process in ship-based CCS', *Energies*, vol. 15, no. 16, p. 5928, Aug. 2022, doi: 10.3390/en15165928.

[19] S. Roussanaly, H. Deng, G. Skaugen, and T. Gundersen, 'At what pressure shall CO_2 be transported by ship? An in-depth cost comparison of 7 and 15 barg shipping', *Energies*, vol. 14, no. 18, p. 5635, Sep. 2021, doi: 10.3390/en14185635.

[20] A. Alabdulkarem, Y. Hwang, and R. Radermacher, 'Development of CO_2 liquefaction cycles for CO_2 sequestration', *Applied Thermal Engineering*, vol. 33–34, pp. 144–156, Feb. 2012, doi: 10.1016/j.applthermaleng.2011.09.027.

[21] D. R. Woods, *Rules of Thumb in Engineering Practice*, 1st ed. Wiley, 2007. doi: 10.1002/9783527611119.

[22] J. Saari, ‘Heat Exchanger Dimensioning’. Accessed: Apr. 26, 2024. [Online]. Available: https://sistemas.eel.usp.br/docentes/arquivos/5817712/LOQ4086/saari__heat_exchanger_dimensioning.pdf

[23] ‘Vapor Liquid Vertical Separator’, CheCalc. Accessed: May 13, 2024. [Online]. Available: https://checalc.com/calc/vertsep.html

[24] ‘Vapor Liquid Separator’, CheGuide. Accessed: Apr. 26, 2024. [Online]. Available: https://cheguide.com/vapor_liquid_separator.html

[25] C. Maxwell, ‘Cost Indices’, Towering Skills. Accessed: Apr. 16, 2024. [Online]. Available: https://toweringskills.com/financial-analysis/cost-indices/

[26] G. P. Towler and R. K. Sinnott, ‘Capital cost estimating’, in *Chemical Engineering Design: Principles, Practice, and Economics of Plant and Process Design*, 2nd ed., Boston, MA: Butterworth-Heinemann, 2013, pp. 307–354.

[27] S. A. Aromada, N. H. Eldrup, and L. Erik Øi, ‘Capital cost estimation of CO_2 capture plant using Enhanced Detailed Factor (EDF) method: Installation factors and plant construction characteristic factors’, *International Journal of Greenhouse Gas Control*, vol. 110, p. 103394, Sep. 2021, doi: 10.1016/j.ijggc.2021.103394.

[28] W. Short, D. J. Packey, and T. Holt, ‘A Manual for the Economic Evaluation of Energy Efficiency and Renewable Energy Technologies’, NREL/TP--462-5173, 35391, Mar. 1995. doi: 10.2172/35391.

[29] H. Yu, D. Kim, and T. Gundersen, ‘A study of working fluids for Organic Rankine Cycles (ORCs) operating across and below ambient temperature to utilize Liquefied Natural Gas (LNG) cold energy’, *Energy*, vol. 167, pp. 730–739, Jan. 2019, doi: 10.1016/j.energy.2018.11.021.

[30] R. Eberhart and J. Kennedy, ‘A new optimizer using particle swarm theory’, in *MHS’95. Proceedings of the Sixth International Symposium on Micro Machine and Human Science*, Nagoya, Japan: IEEE, 1995, pp. 39–43. doi: 10.1109/MHS.1995.494215.

[31] M. A. El-Shorbagy and A. E. Hassanien, ‘Particle swarm optimization from theory to applications’, *International Journal of Rough Sets and Data Analysis*, vol. 5, no. 2, pp. 1–24, Apr. 2018, doi: 10.4018/IJRSDA.2018040101.

[32] A. Andreasen, ‘Optimisation of carbon capture from flue gas from a Waste-to-Energy plant using surrogate modelling and global optimisation’, *Oil Gas Sci. Technol. – Rev. IFP Energies nouvelles*, vol. 76, p. 55, 2021, doi: 10.2516/ogst/2021036.

[33] E. R. Olsen, J.-O. Hooghoudt, M. Maschietti, and A. Andreasen, 'Optimization of an oil and gas separation plant for different reservoir fluids using an evolutionary algorithm', *Energy Fuels*, vol. 35, no. 6, pp. 5392–5406, Mar. 2021, doi: 10.1021/acs.energyfuels.0c04284.

[34] J. van Baten, 'ScanIt', AmsterCHEM. Accessed: May 13, 2024. [Online]. Available: https://www.amsterchem.com/scanit.html

7 Appendix A: Simulations in Aspen HYSYS

7.1 Simulations of Base Cases

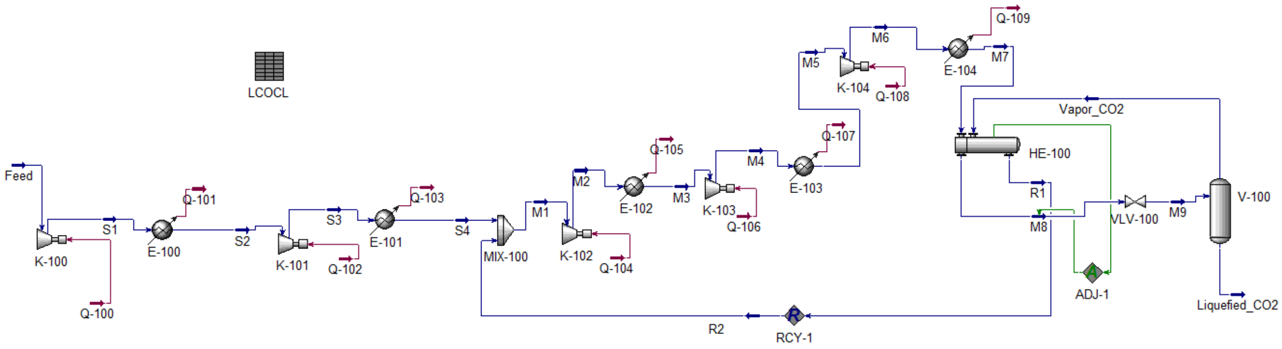

Figure 10. Aspen HYSYS simulation of Internal refrigeration at 7 bar.

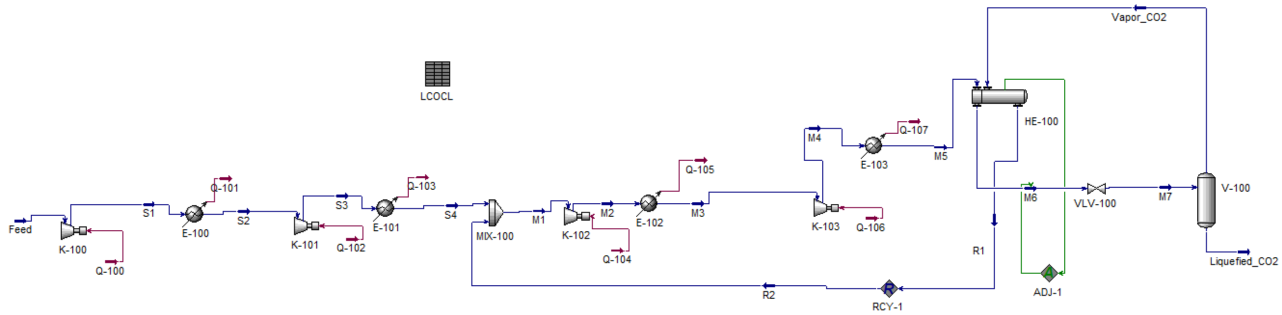

Figure 11. Aspen HYSYS simulation of Internal refrigeration at 15 bar.

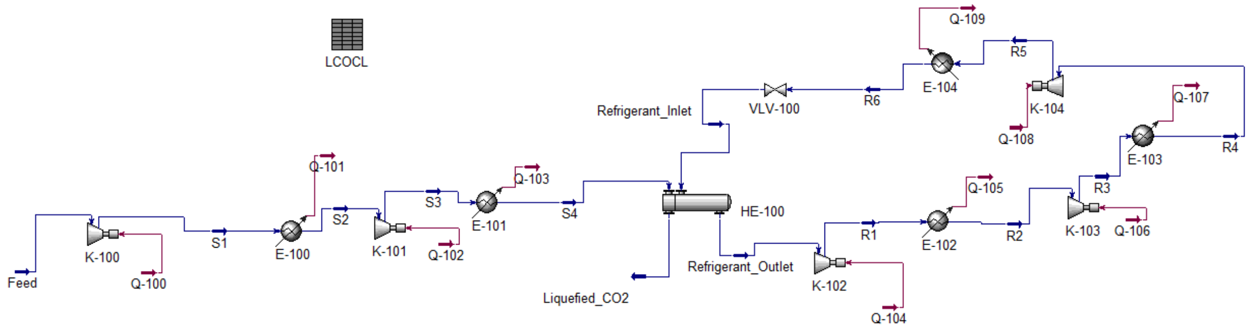

Figure 12. Aspen HYSYS simulation of External refrigeration at 7 bar.

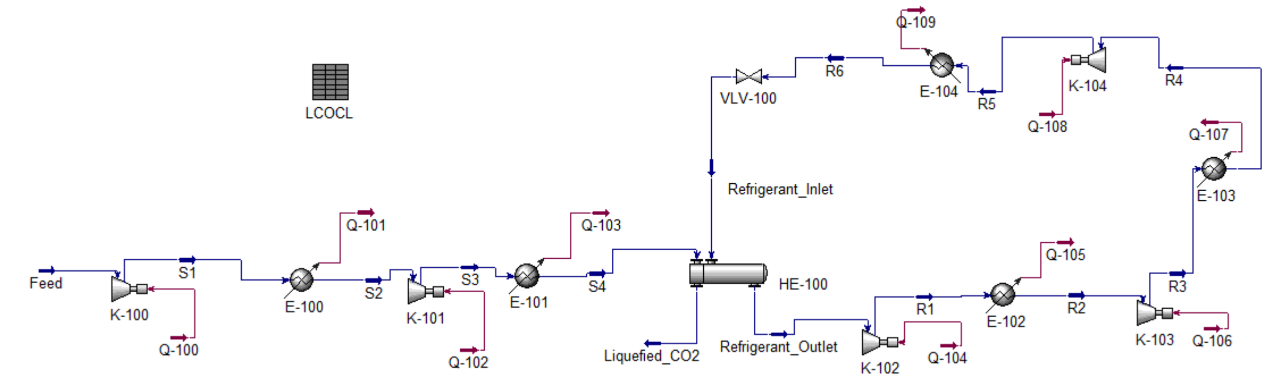

Figure 13. Aspen HYSYS simulation of External refrigeration at 15 bar.

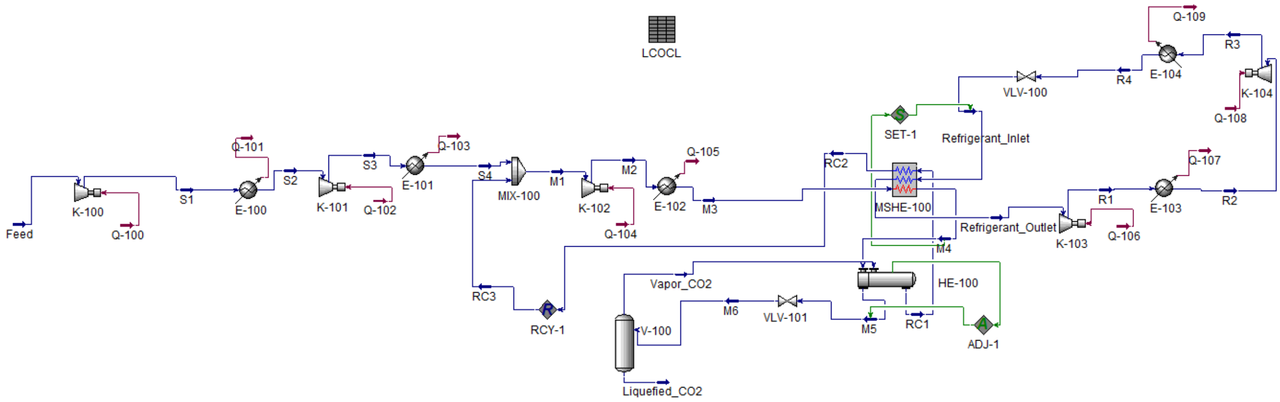

Figure 14. Aspen HYSYS simulation of precooled Linde-Hampson system at 7 bar.

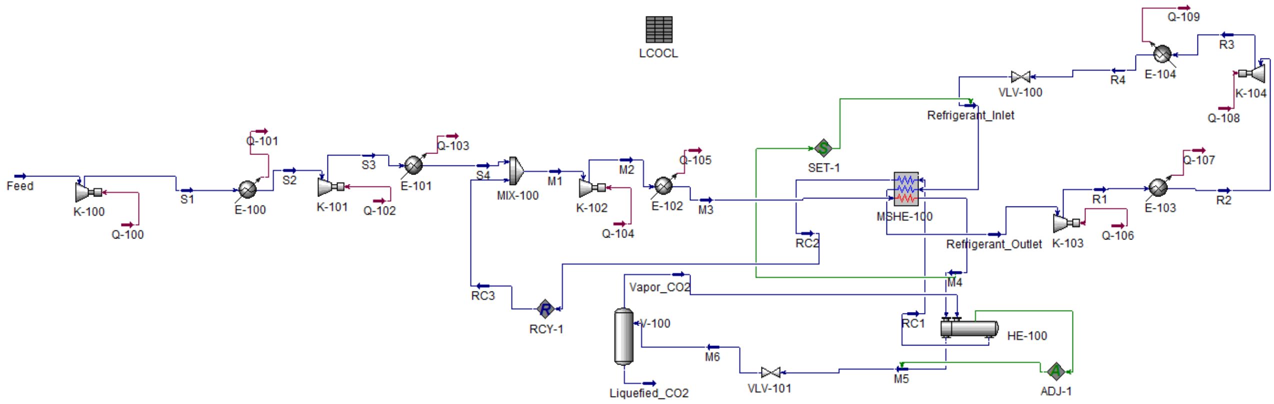

Figure 15. Aspen HYSYS simulation of precooled Linde-Hampson system at 15 bar.

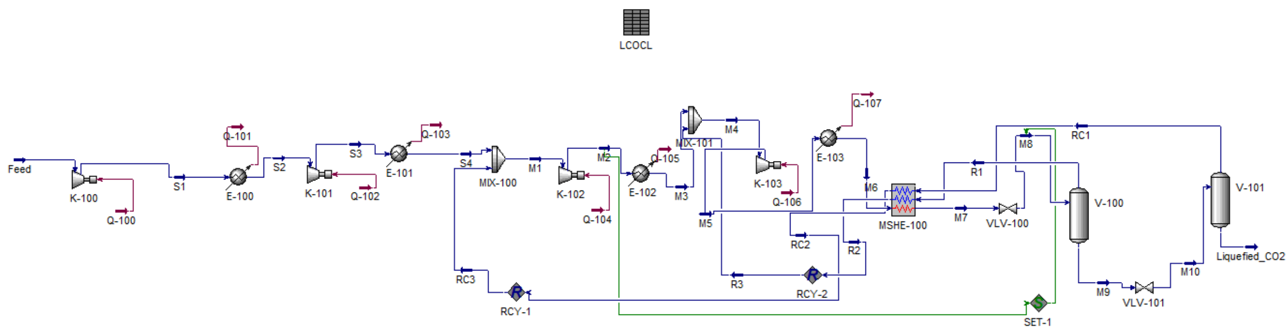

Figure 16. Aspen HYSYS simulation of Linde dual-pressure system at 7 bar.

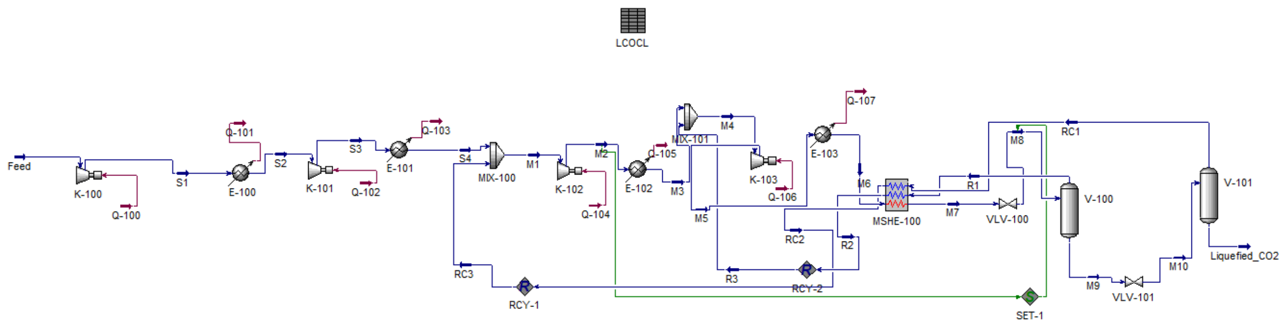

Figure 17. Aspen HYSYS simulation of Linde dual-pressure system at 15 bar.

7.2 Simulation of Case B

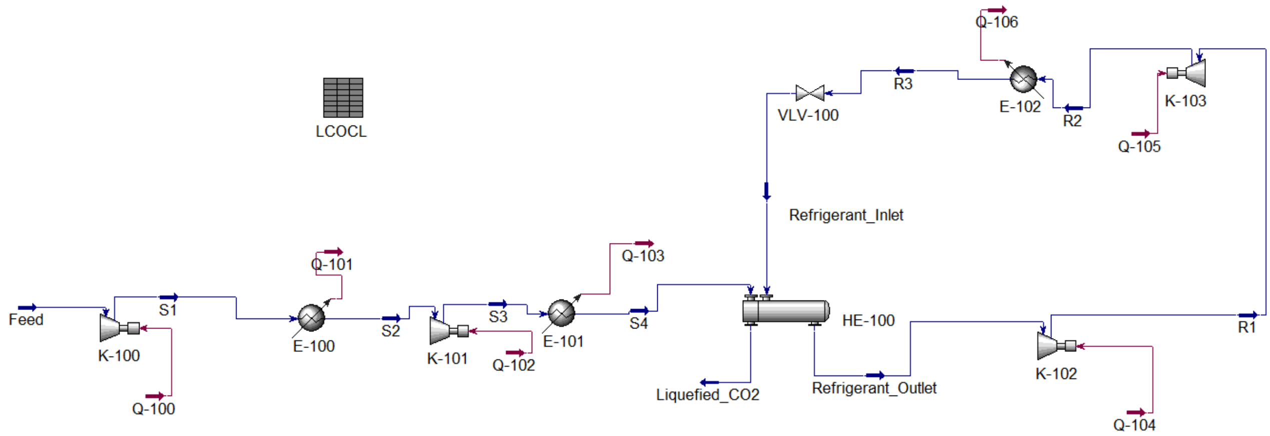

Figure 18. Aspen HYSYS simulation of Case B.

7.3 Simulation of Case C

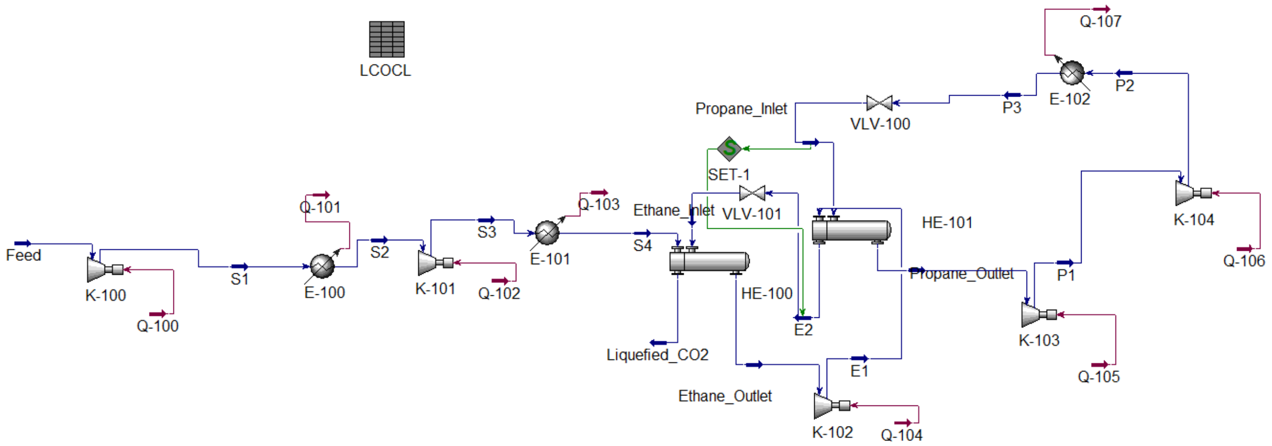

Figure 19. Aspen HYSYS simulation of Case C.

7.4 Simulations of Case D

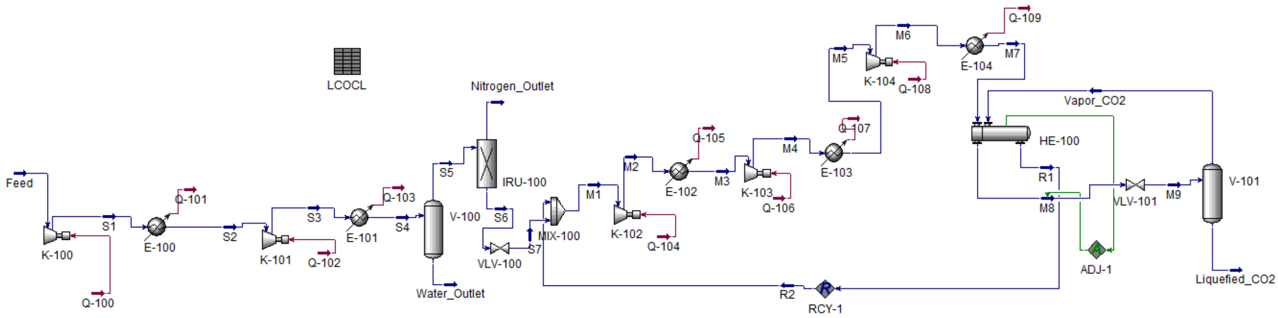

Figure 20. Aspen HYSYS simulation of Case D, Internal refrigeration at 7 bar.

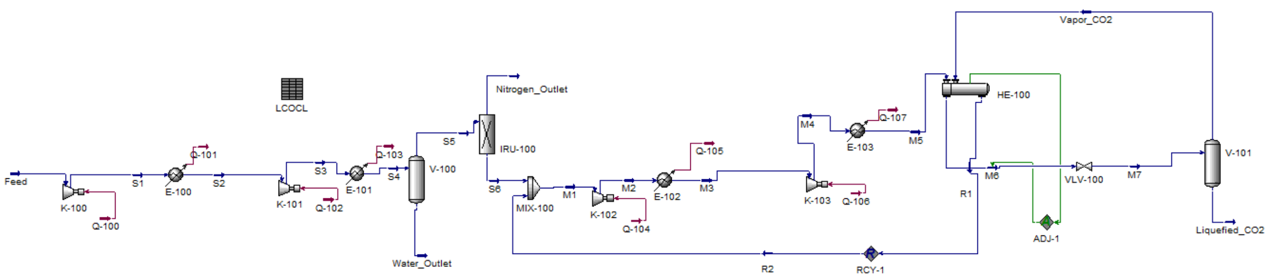

Figure 21. Aspen HYSYS simulation of Case D, Internal refrigeration at 15 bar.

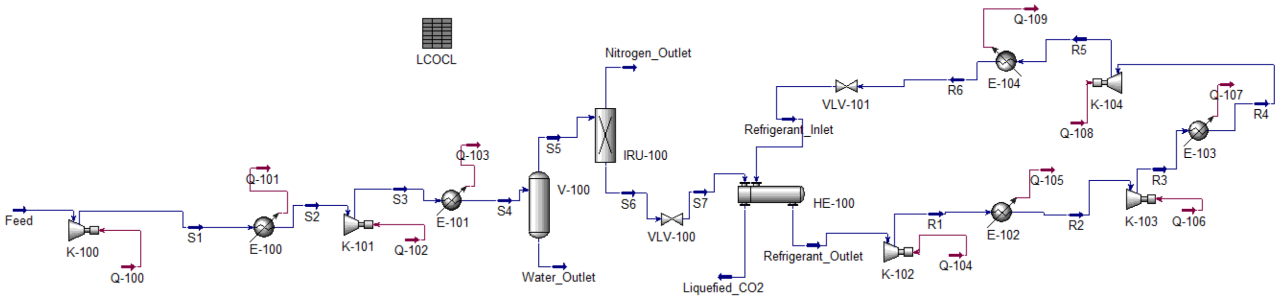

Figure 22. Aspen HYSYS simulation of Case D, External refrigeration at 7 bar.

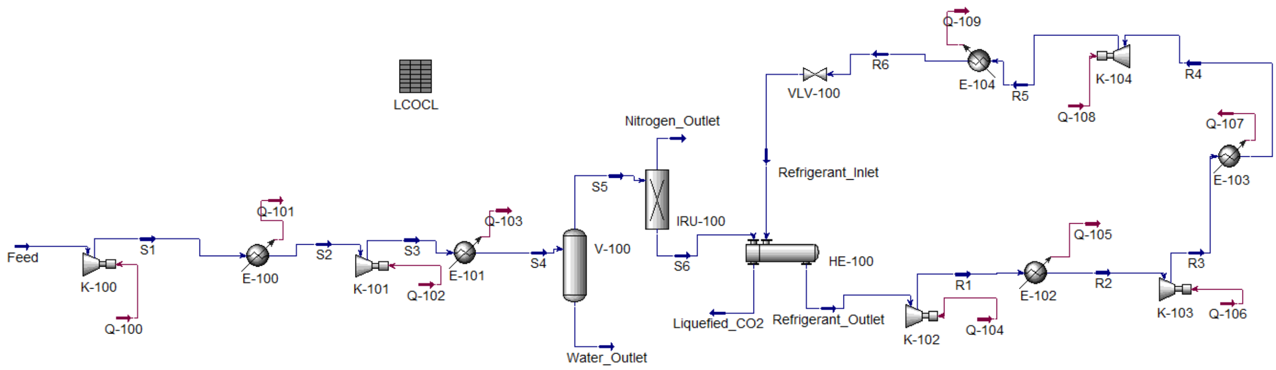

Figure 23. Aspen HYSYS simulation of Case D, External refrigeration at 15 bar.

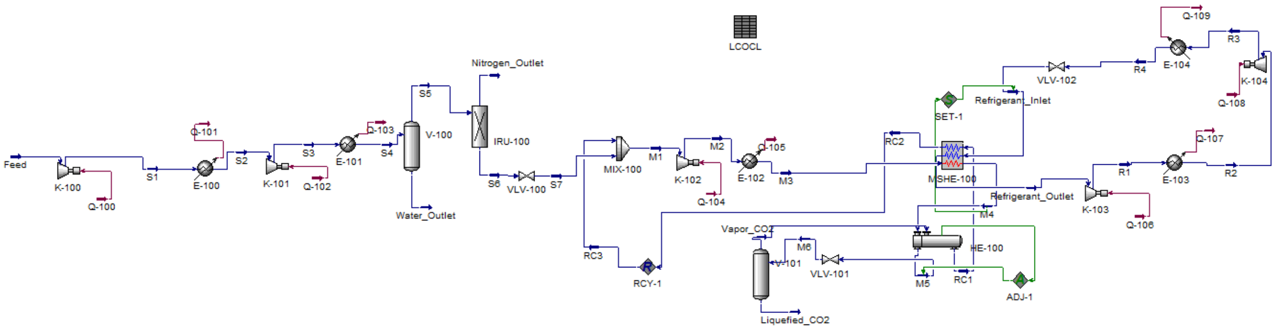

Figure 24. Aspen HYSYS simulation of Case D, precooled Linde-Hampson system at 7 bar.

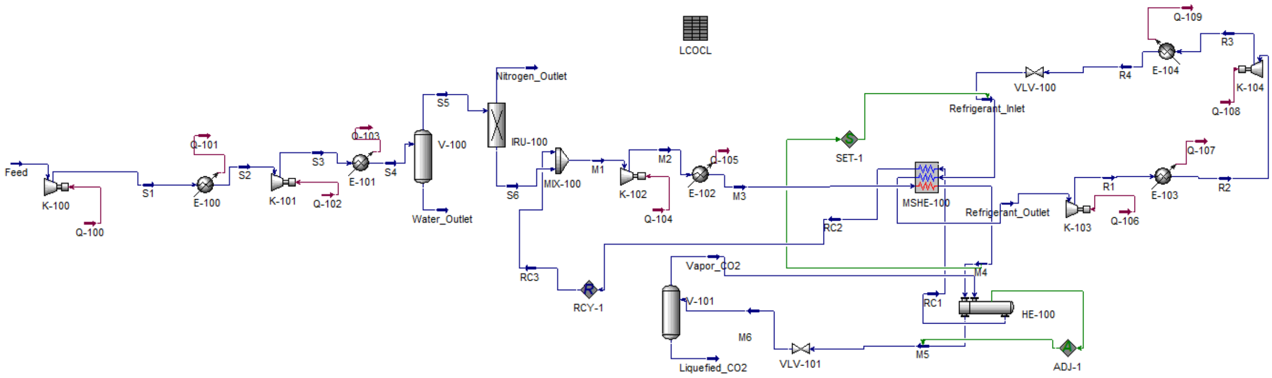

Figure 25. Aspen HYSYS simulation of Case D, precooled Linde-Hampson system at 15 bar.

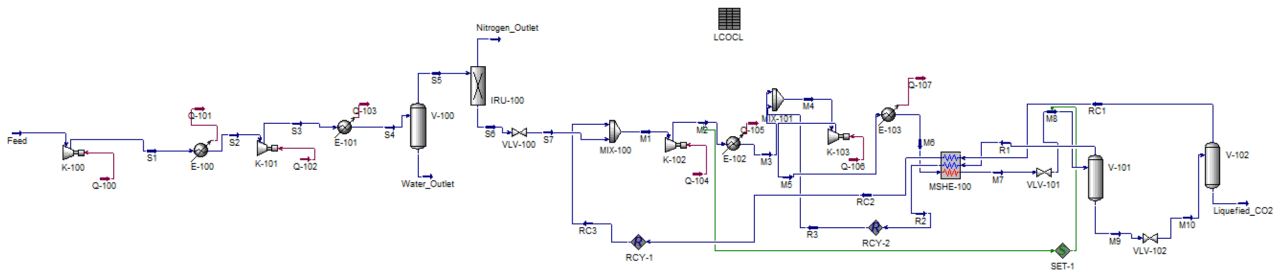

Figure 26. Aspen HYSYS simulation of Case D, Linde dual-pressure system at 7 bar.

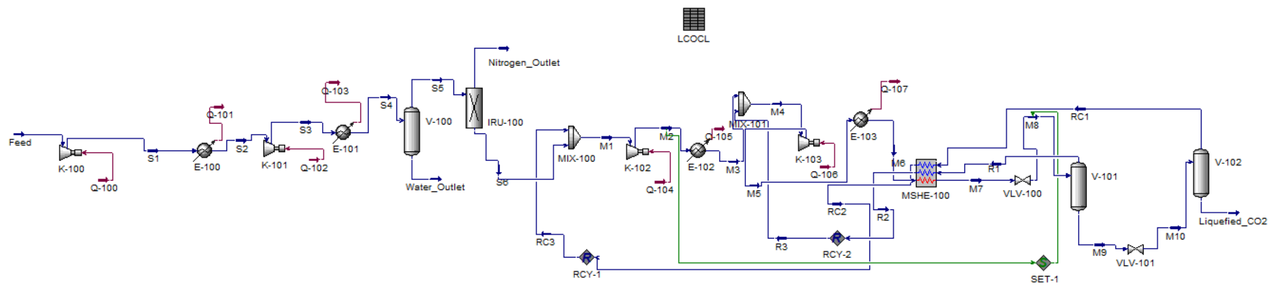

Figure 27. Aspen HYSYS simulation of Case D, Linde dual-pressure system at 15 bar.